STARS

University of Central Florida
STARS

Retrospective Theses and Dissertations

1988

Laser induced darkening semiconductor dope glasses

Jayant Malhotra
University of Central Florida

LASER INDUCED DARKENING IN SEMICONDUCTOR DOPED GLASSES

BY

JAYANT MALHOTRA
B.Tech., Indian Institute of Technology, 1986

THESIS

Submitted in partial fulfillment of the requirements
for the degree of Master of Science
in the Graduate Studies Program
of the College of Engineering
University of Central Florida
Orlando, Florida

Fall Term
1988

ABSTRACT

Darkening and other aging effects in semiconductor doped glasses due to laser irradiation have been reviewed. Experiments were performed to characterize darkening. Measurements were made as a function of fluence, repetition rate and pulsewidth using a picosecond, frequency doubled Nd:YAG laser. Darkening was found to increase rapidly during initial stages of laser irradiation and then level off, after which no further change was observed. The final extent of darkening was greater for larger fluence. For a given fluence, stronger darkening was produced at a pulsewidth of 100 ps than at 30 ps. This indicates a two step absorption with a fast relaxation at intermediate levels as a possible mechanism for electron trapping.

ACKNOWLEDGEMENTS

TABLE OF CONTENTS

CHAPTER 1

INTRODUCTION

1.1 Scope and Layout of Thesis

Semiconductor doped glasses have been actively studied for the last several years. They have been shown to have strong nonlinearity and fast nonlinear response. However, aging due to continuous laser irradiation is known to change their properties. A darkening or drop in transmission also occurs due to aging. The exact mechanism behind these is not known.

Experiments were performed to characterize darkening as a function of fluence, repetition rate and pulse width. The experimental arrangement and results have been discussed in Chapter 3. In Chapter 1, the importance of optics in modern technology has been discussed. A brief review of nonlinear optics and Degenerate Four Wave Mixing (DFWM) has been done. DFWM was used by other experimenters to measure carrier decay times. In Chapter 2, review of manufacturing process, quantum confinement studies and nonlinear studies done by other experimenters has been done. Finally conclusions and suggestions of possible mechanisms behind darkening have been made in Chapter 4.

1.2 Optics and Technology

Usage of light to transmit and process information is among the latest and fastest developing technology areas. While optical methods have become an efficient and reliable means of voice and data communication, processing data optically is still a developing science and at this time, an actively researched area [1, 2, 3, 4, 5].

Optical techniques have the following fundamental advantages over electronics:

1. Light is an inherently parallel transmission media. This could lead to transmitting large amounts of data and make high degrees of interconnectivity possible. This would also allow a very high degree of parallel processing [1].

2. Optical devices with high switching speeds (subnanosecond or even subpicosecond) are possible, this would lead to fast processing rates [3].

3. All optical devices are much more immune to electromagnetic interference from electrically noisy industrial environments.

4. Possible to implement advanced algorithms like fast Fourier transforms with a greater ease due to special properties of light, which are difficult to implement in present VLSI based digital systems. However, these only apply to analog processors so far [6].

Among the several constraints encountered, the development of an optical switch is a primary one. The ideal optical switch would need a material that has strong nonlinearity and fast nonlinear response. Several nonlinear materials are known. Indium Antamonide has been studied and it shows strong optical nonlinearity at low temperature (77 K) [8]. Multiple Quantum Wells of GaAs/GaAlAs have also been researched and show good promise [7]. Other known optically nonlinear materials are CdS [8], $CdS_x Se_{1-x}$ doped glass [19], $Cd_{0.23} Hg_{0.77} Te$ [9], ZnS [10], ZnSe [11], Na [12], CS_2 [13], Nitrobenzene [13], Dye [14] etc. Among these, $CdS_x Se_{1-x}$ doped glasses are of great interest.

1.3 Nonlinear Optics

The polarization induced in a material in the presence of an optical field is

$$P(E) = \chi E .$$

where χ is the optical susceptibility. This is usually a constant, but at higher intensities the linear relationship between P and E breaks down and the susceptibility

now depends on the applied optical field [15]. It can be expanded mathematically as :

$$\chi(E) = \chi^{(1)} + \chi^{(2)} E + \chi^{(3)} E^2 + ...$$

The polarization of the material is found by multiplying E times $\chi(E)$:

$$P(E) = \chi(E)E = \chi^{(1)} E + X^{(2)} E^2 + \chi^{(3)} E^3 + ...$$

E denotes the total electric field and as seen from the above expression the polarization P depends upon higher powers of electric field. The total electric field is usually made up of a number of different waves at different frequencies, polarizations, k vectors, etc. Thus there are usually many terms in the expression for E (and more for E^2). For this reason each χ in the previous expansion has several components each a function of frequency. In the above expression such nature of E and χ is implied.

$\chi^{(1)}$ corresponds to linear optical properties including index of refraction, absorption, gain and birefringence. These properties constitute the subject of classical optics, and these coefficients cannot be responsible for the production of a conjugate wave because a nonlinear process is needed to couple waves in material.

The $\chi^{(2)}$ terms in equation corresponds to second order effects, which in general, can be called three wave mixing. These effects are:

second harmonic generation

optical rectification

parametric mixing.

These effects occur only in materials that lack inversion symmetry.

The $\chi^{(3)}$ effects may occur whether or not the material possesses inversion symmetry. Most well known of these χ^3 effects are:

stimulated Brillouin scattering

stimulated Raman scattering

nonlinear refraction

two photon absorption.

1.2.1 Optical Phase Conjugation and Degenerate Four Wave Mixing

Optical phase conjugation (OPC) is a phenomena which causes the direction and phase of an incident wave to be reversed [15]. An ordinary mirror will reflect an incident wave at a reflecting angle such that the angle of incidence is equal to angle of reflection. A phase conjugate mirror will reflect a beam backwards along the incident direction. Optical phase conjugation can occur due to stimulated Brillouin scattering, stimulated Raman scattering and nonlinear absorption or refraction. One important method of producing conjugate waves is via degenerate four wave mixing (DFWM).

The DFWM geometry consists of irradiating the nonlinear sample by two plane pump waves. See Figure 1. E_f and E_b are the forward and backward pumps, both are counter propagating along the x axis. E_p is the probe wave, and is the wavefront of which we wish to generate the conjugate. It is incident at an angle θ to the x axis. E_c is the conjugate of E_p also at the same frequency.

The optical signal frequency is usually chosen such that it is resonant or nearly resonant with atomic or molecular transitions in the nonlinear medium. Because E_p, E_f, E_b all oscillate at the same frequency ω, they interfere to form a spatial intensity modulation pattern.

Two important modulation patterns in the case where E_p is also a plane wave are shown in the Figure 2. E_p and E_f form a grating of relatively large period in which the important Fourier component is exactly phase matched to Bragg scattering E_b to E_c, the phase conjugate of E_p. E_p and E_b on the other hand form a finer grating
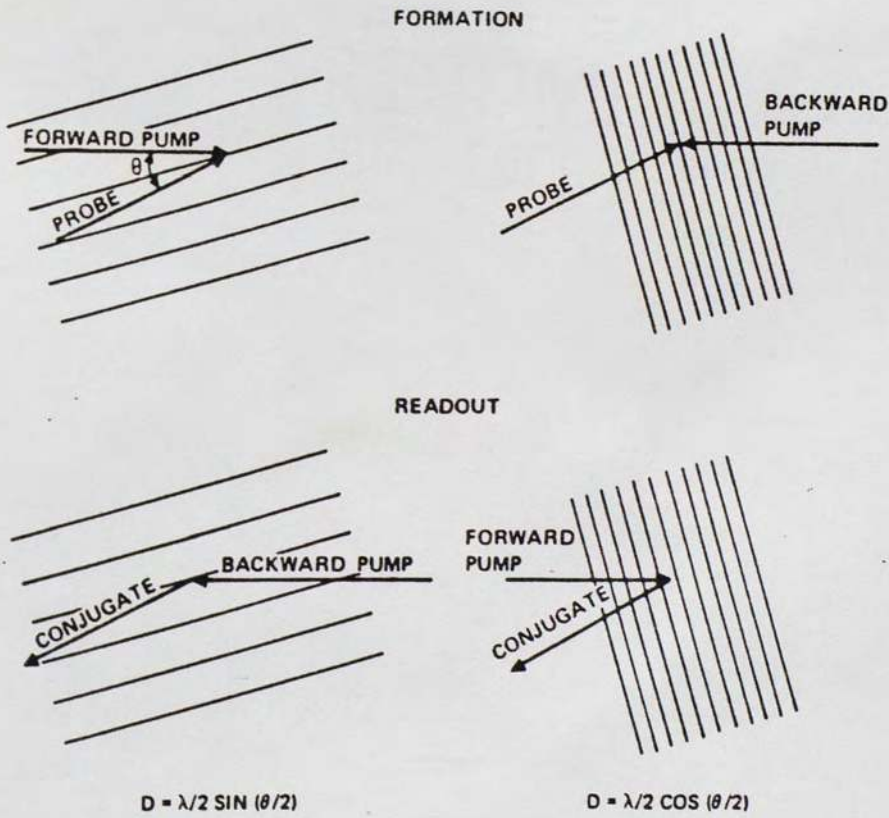
Figure 2. The grating picture.

Figure 1. The DFWM geometry.

and spacing and orientation to similarly scatter E_f into E_c. A third grating due to the interference of E_f and E_b does not contribute to the process, because it is not phase matched for scattering of E_c or E_p. See Figure 2.

The basic theory of phase conjugation by four wave mixing is presented as follows [16]. The third order nonlinearity can be written as below:

$$P_i = 4\chi_{ijkl} \ E_j \ E_k \ E_l$$

The complex amplitude of the induced polarization at the frequency $\omega_1 = \omega_2 + \omega_3 - \omega_4$ is related to the electric field amplitudes according to:

$$P_i \ (\omega_1 = \omega_2 + \omega_3 - \omega_4) = 6\chi_{ijkl} \ (-\omega_1 ,\omega_2 ,\omega_3 ,-\omega_4) \ E_j \ (\omega_2) \ E_k \ (\omega_3) \ E_l^* \ (\omega_4)$$

Refer to Figure 1. The pump waves are taken as:

$$E_{f,b} = A_{f,b} \ (r) \ \exp \ i(\omega t - k_f , k_b .r)$$

The waves E_c , E_p are not plane waves in general. E_p is considered some kind of input wave and E_c as the output. The four waves are coupled by means of the nonlinear polarization. Consider the nonlinear polarization term due to the mixing of the frequency degenerate waves E_f , E_b , E_p :

$$P_{NL}{}^{\omega=\omega+\omega-\omega} \ (r,t) = \frac{1}{2} \ \chi^{(3)} \ A_f \ A_b \ A_p^* \ \exp \ i[(\omega+\omega-\omega)+(k_f +k_b).r +k_p \ z]$$
$$= \frac{1}{2} \ \chi^{(3)} \ A_f \ A_b \ A_p^* \ \exp \ i(\omega t+k_p \ z)$$

since $k_f + k_b = 0$. The above equation corresponds to a polarization wave with a frequency ω and a wave with a wave vector $k_c = -k_p$ and this will excite a wave E_c of the form :

$$E_c = A_c \ (z) \ \exp \ i(\omega t+k_c \ z)$$

E_c will mix with the pump waves to generate a polarization:

$$P_{NL}{}^{\omega+\omega-\omega} \ (z,t) = \frac{1}{2} \ \chi^{(3)} \ A_f \ A_b \ A_p^* \ \exp \ i(wt-k_c \ z)$$

which has the same frequency and propagation vector as E_p so that it will interact strongly with this wave. This is how the interaction and power exchange of E_p and E_c is mediated via the pump waves.

Starting with the basic coupling equation of a wave to a nonlinear polarization we get:

$$-ik \frac{dA_c}{dz} \exp i(\omega t + kz) = -\mu_o \frac{\partial^2}{\partial t^2} [P_{NL}{}^\omega (z,t)]$$

Using the equation for P_{NL} we get

$$\frac{dA_c}{dz} = i \frac{\omega}{2} \sqrt{\frac{\mu_o}{\epsilon}} \chi^{(3)} A_f A_b A_p{}^*$$

and similarly

$$\frac{dA_p{}^*}{dz} = i \frac{\omega}{2} \sqrt{\frac{\mu_o}{\epsilon}} \chi^{(3)} A_f{}^* A_b{}^* A_c$$

Using $\kappa^* = \frac{\omega}{2} \sqrt{\frac{\mu_o}{\epsilon}} A_f A_b \chi^{(3)}$ and solving the equations at z=0 we obtain:

$$A_c (0) = -i \left[\left(\frac{\kappa^*}{|\kappa|} \right) \tan|\kappa|L \right] A_p{}^* (0)$$

One important application of DFWM is the measurement of the temporal decay of the transient gratings formed. In this case laser pulses much shorter than the decay time of interest must be used. For example, in intermediate gap semiconductors the decay times are typically nanoseconds so that picosecond pulses must be used. Usually three pulses E_p , E_f , E_b arrive at the same time, but a pulse say E_b can be made to come at a delay using a delay line. If the lifetime of the grating is longer than the delay, a conjugate signal can be observed, but if it is smaller, small conjugate signal can be observed. Thus by changing delay times, the temporal decay of E_f and E_p gratings can be observed. The grating lifetimes are indicative of the nonlinear response times of the material. This is a very important parameter and DFWM is commonly used to measure it.

CHAPTER 2

SEMICONDUCTOR DOPED GLASS : A REVIEW

2.1 Introduction

The glasses discussed are silicate glasses in which $CdSe_x S_{1-x}$ microcrystalline phase is thermally developed [17, 18]. These glasses are easily available commercially as sharp cutoff filters. The value of x determines the band gap and hence the cut off point. They are available from yellow to red wavelengths. Typically in the Corning glasses, the diameter of the microcrystals in these glasses is around 100A.

2.1.1 Commercial Availability

The glasses are manufactured by Schott and Corning. We had both Schott and Corning samples available to us. The Schott glasses have a uniform numbering system. The absorbtion edges range from 400 nm to 665 nm. Refer to the data available on it. The glass type code has two letters followed by a three digit number. The first letter roughly indicates the color of the glass, i.e., red orange or green and last three digits give the absorption edge wavelength in nanometers. Corning glasses made available had a more complicated identification system. The samples also had varying thicknesses. The absorption edge wavelength versus glass number is given in Table 1.

2.1.2 Manufacturing Process

These glasses are manufactured by adding a few weight percent of Cadmium, Selenium and Sulfur (in the form of CdO, CdS and elemental Sulfur or Selenium) to the batch materials of what would otherwise be a transparent silicate glass [17, 18].

TABLE 2

Yellow, Orange and Red Sharp Cut-Off Glass Filters.

Schott Glass Type	$\Delta\lambda$ ΔT	Correction Factor $(t_1 t_2)$	PRODUCT NUMBER
GG 400	0.07	0.91	03 FCG 057
GG 420	0.07	0.91	03 FCG 059
GG 435	0.07	0.91	03 FCG 061
GG 455	0.08	0.915	03 FCG 063
GG 475	0.09	0.915	03 FCG 065
GG 495	0.10	0.915	03 FCG 067
OG 515	0.11	0.915	03 FCG 083
OG 530	0.12	0.915	03 FCG 085
OG 550	0.13	0.915	03 FCG 087
OG 570	0.14	0.915	03 FCG 089
OG 590	0.15	0.915	03 FCG 098
RG 610	0.16	0.915	03 FCG 101
RG 630	0.17	0.915	03 FCG 103
RG 645	0.17	0.915	03 FCG 105
RG 665	0.17	0.915	03 FCG 107

$\frac{\Delta\lambda}{\Delta T}$ is the temperature coefficient of half-power point position shift, in nm $^\circ C^{-1}$
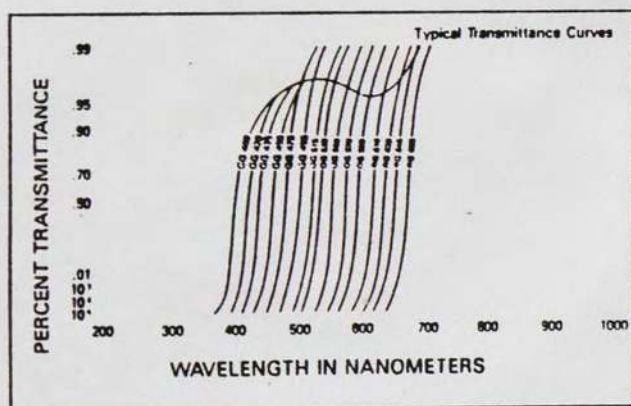

Figure 3. Typical transmittance curves
for sharp cut off filters.

The batch is typically melted within the range of 1300-1400 °C and formed by conventional techniques. Furthermore annealing is done at 450-550 °C to produce a stress free optical quality glass. Subsequently the glass is heat treated with a peak temperature in the range 575-750 °C for a duration of 0.5 to 4 hours. This process produces the microcrystalline phase.

In general the higher the heat-treament temperature and the longer the treatment time, the larger is the average crystallite size and the larger the number density of particles. The process of crystal growth is due to a ripening or coarsening effect. In such a system larger particles are unstable with respect to the degree of supersaturation and grow by precicipation of solute from the matrix, while smaller particles, also unstable with respect to the solute concentration, dissolve back into the matrix. The coarsening process is mainly observed in the later stages of the precipitation process when no further nucleation of new particle occurs because supersaturation of the matrix with respect to the solute atoms has become very small.

For the $CdS_x Se_{1-x}$ there is also a gradual change in crystal stoichiometry during growth process, an increase in Se concentration. This is due to a large difference in diffusion coefficient in the glass between Sulfur and Selenium.

2.2 Quantum Confinement Studies

In addition to its optical nonlinearity, semiconductor doped glasses are also important from the point of view of quantum confinement studies. The semiconductor doped glass may be a useful way to study the effect of quantum confinement of the electron and hole wavefunctions by a deep potential well on the excitonic and band gap energy structure.

2.2.1 Absorption Spectrum

Absorption spectrum of samples of CdS and CdSe glasses were measured by Borelli et al [17]. See Figures 4, 5. In both figures the (a) part shows spectra of samples heat treated for 0.5 h at various temperatures. The (b) part shows curves of samples treated at one temperature 593 °C for CdSe glass and 600 °C for the CdS glass for different durations.

As mentioned earlier higher temperature or longer heat treatment times lead to crystals of larger diameter. From the figures it is clear that as the crystal diameter becomes smaller there is a blue shift in the absorption edge. Due to reduced size the energy of the particles in the potential well increases, and this increase can lead to the observed short wavelength shift. The peakss observed at the absorption edge are believed to be due to excitons [17, 33].

2.2.2 Photoluminescence

Photoluminescence spectra of the CdSe glass are shown in Figure 6 [18]. These figures shed more evidence on quantum confinement behaviour. The spectra consists of two bands, a less intense high energy band, denoted as peak 1 and a lower energy broader band denoted peak 2. The first peak occurs in each sample at a wavelength 10 - 20 nm greater than the absorption edge and is due to direct electron - hole recombination. The peak shifts towards larger wavelengths with increasing particle size.

Consider a 700/0.5 sample; it has absorption edge and luminiscence peak 1 at 687 and 676 nm. While bulk crystal band gap of CdSe λg is at 721 nm. The slight shift towards higher energy may be the result of a small degree of quantum confinement with unresolved absorption features or because of uncertainity in bulk crystal band gap determination experiment.

Figure 4. Absorption spectra of the CdSe experimental glass for samples with heat treatments of 0.5 h and various temperatures (a) and for samples with a treatment at 593 °C for various durations (b). Ref. [17].

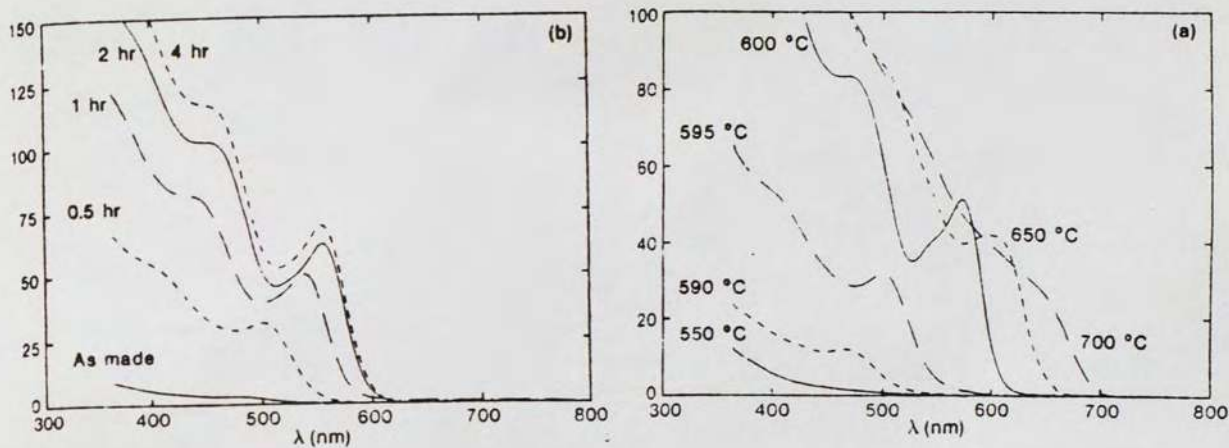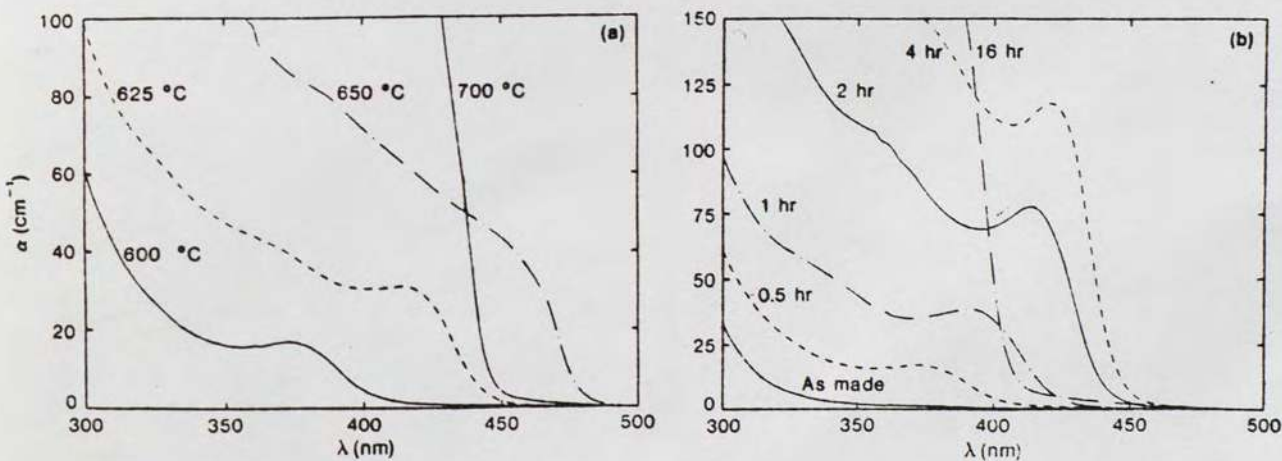Figure 5. Absorption spectra of the CdS experimental glass for samples with heat treatments of 0.5 h and various temperatures (a) and for samples with a treatment at 600 °C for various durations (b). Ref. [17].
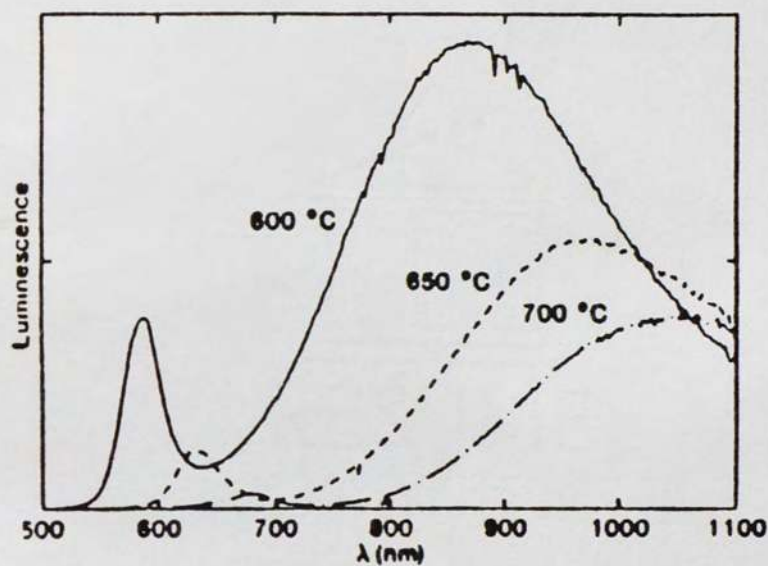
Figure 6. Luminescence spectra of samples of the experimental CdSe glass which recieved heat treatment of 0.5 hour at the temperature indicated. Ref. [18].

The intensity of the second peak is much higher than the first peak. The short wave shift is consistant for both the peaks. The ratio of peak 1 to peak 2 decreases with increasing particle size. The second peak is due to recombination through intermediate states which may be impurity levels or surface states. As particle size decreases, more recombination occurs via intermediate states than direct recombination.

2.2.3 Theory

Efros and Efros [27] dilineate the situation into three separate sphere size regimes dependent upon the size of the dielectric sphere (R) and its relationship to the Bohr radii of the carriers (a_e and a_h). An interband absorption threshold energy is then calculated through an evaluation of transition probabilities for the different regimes. The two extreme cases are shown as:

$$\hbar\omega = E_g + \left[\frac{h^2 \pi^2}{2\mu^2 R^2}\right] \quad \frac{1}{\mu} = \frac{1}{m_e} + \frac{1}{m_h} \quad R < a_h < a_e$$

$$\hbar\omega = E_g - E_{ex} - \left[\frac{h^2 \pi^2}{2M^2 R^2}\right] \quad M = m_e + m_h \quad a_h < a_e < R$$

From above it can be seen that if a plot of energy versus $1/R^2$ was done [18]. See Figure 7. The slope would be decided by effective mass. There is also a coulombic interaction between carriers. In the studies done by Potter et al. of CdS crystals from 40 to 400 °A there was a clear inverse square size dependence in both the absorption edge and photoluminescence peak. From the data collected, the effective mass calculated was only about 10-30 times lower than the exciton translational mass predicted by Efros and Efros.
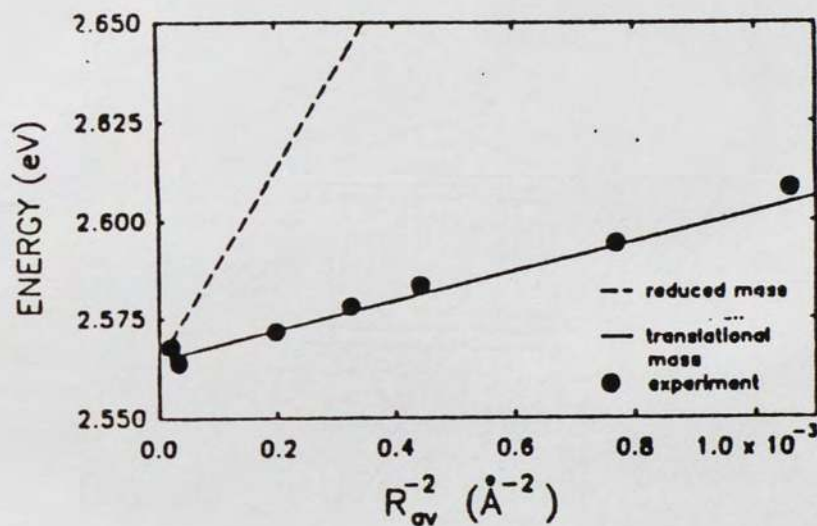
Figure 7. The lowest excited-state energy plotted as a function of the inverse average square crystallite radius using the Efros and Efros first and third size regime interpretations . Experimentally observed absorption threshold energies are also included for the CdS glass composite. Ref.[18].

Quantum confinement effects have a variety of applications since they lead to an increase in excitonic binding energy. This will let excitonic levels remain distinct at higher temperatures.

This phenomena is important for nonlinear processes which utilize resonant excitonic transitions and state filling effects to induce a large rapid change in refractive index of a crystal with a subnanosecond decay time.

2.3 Optical Nonlinear Study

Nonlinear optical study of semiconductor doped glasses has been of great interest in the last few years.

2.3.1 Initial Studies

Optical phase conjugation by DFWM was first studied by Jain and Lind [19]. They reported a very large third order susceptibility χ^3 of with a fast (subnanosecond) response. For their experiments they chose several glasses with different absorption edge and selecting wavelengths in the cutoff region.

TABLE 2

Wavelength (nm)	Glass composition (Sulfur fraction)	Representative glass	χ^3 measured
532.0	0.9	Corning 3484 CS-3-68	1.3×10^{-8}
580.0	0.7	Corning 2434 CS-2-73	5×10^{-9}
694.3	0.1	Schott RG 695	3×10^{-9}

Pump intensities used are approximately 1 MW/cm² ; pulsewidth used was approximately 10 ns.

DFWM experiments were done on bulk CdS and semiconductor doped glass Corning 3484 (CS-3-68) for the sake of comparison between bulk semiconductor and

microcrystallites. At an intensity of 1 MW/cm² the χ^3 measured were the same but the glass had a faster response. At lower intensities of 0.1 MW/cm² CdSSe glass showed a much larger χ^3 than the bulk semiconductor. The authors suggest that this could be because of better match of frequency with the absorption edge.

K.C. Rustagi and C. Flytzanis [20] have suggested an explanation. Using Maxwell Garnett theory [32], and modification of dielectric function approach [15]. The model composite material consists of spherical inclusions of one medium of dielectric constant ϵ_1 in another medium of ϵ_2, p denotes the fractional volume occupied by the dopant and ϵ_c the dielectric constant for the composite material. They arrived at an expression for modification $\Delta\epsilon_c$ of ϵ_c.

$$\Delta\epsilon_c = \frac{-9\epsilon_2{}^2}{\left[(1-p)\epsilon'_1+(2+p)\epsilon_2\right]^2} \; \frac{4\pi e^2}{m_{eh}\;\omega^2} \; \frac{\omega_g{}^2}{[\omega_g{}^2-\omega^2]} \; \frac{[\eta\alpha_c\;\tau I]}{[\hbar\omega]}$$

where ω_g is the band gap frequency, $\hbar\omega_g = E_g$, η = quantum efficiency, α_c = absorption coefficient of the composite material, m_{eh} = reduced mass of electron - hole pair and τ = recombination time.

When this expression is compared with corresponding relation for homogeneous semiconductors.

$$\Delta\epsilon_1 = \frac{-4\pi e^2}{m_{eh}\;\omega^2} \; \frac{\omega_g{}^2}{[\omega_g{}^2-\omega^2]} \; \frac{\eta\alpha_1\;\tau I}{\hbar\omega}$$

where $\alpha_1 = p\;\alpha_c$.

It can be observed that for equal absorption the induced change $\Delta\epsilon$ is about the same in the two cases. $(\omega_g{}^2 - \omega^2)$ is smaller by a factor of 8 for the Corning 3484 filter. If τ and m_{eh} are equal for the two samples, we can then estimate that the

optimized DFWM signal from the colored glass should be larger by a factor of 10 in the low intensity regime. Jain and Lind observed that the DFWM signal from a glass filter was four times larger than that from CdS and there was a much slower ($\simeq I^{0.9}$) dependence on pump intensity.

At I= 1 MW/cm² , the density of generated carriers is estimated to be 0.8×10^{18} cm^{-3} for τ= 1 ns. The fact that Jain and Lind did not observe any saturation of absorption at such a high density of particles strongly suggests additional absorbtion by the generated carriers. This could mask the saturation of absorption resulting from valence to conduction band transitions and also modify the energy distribution of carriers.

If the local density of generated carriers is indeed the primary parameter that determines saturation, it follows that the saturation can be reduced and that the DFWM signal can be increased by increasing p and the sulphur fraction x together so as to keep α a constant.

Jain and Lind rule out simple saturation effects as reason for nonlinearity. In their experiments the photon energy (2.3 eV) was sufficiently small compared with the estimated band gap (2.4 eV).

They also rule out thermal mechanisms. Thermal gratings may easily result in large DFWM signals; however, they are characterized by long time constants typically of the order of microseconds. In the experiments by Jain and Lind, the DFWM signals were observed to decay rapidly with pulse delay, measurement of decay time being limited by the pulse widths. This observation indicates that nonlinearity is much faster than the laser pulse duration and that it cannot be attributed to a thermal mechanism.

Jain and Lind believe that generation of a electron-hole plasma by interband absorption of the laser radiation is a plausible source of nonlinearity. The value of χ^3

is equal to 1.3×10^{-8} obtained for CdSSe (Corning glass 3484 color filter no. CS-3-68). This value is in order of magnitude agreement with plasma generation model.

2.3.2 Comparison of Schott OG 530 and Corning 3-68

In a later paper by Ruossignol et al. [21], study of optical phase conjugation was done in the same materials. They studied Corning 3-68 (also studied by Jain and Lind) and OG 530, an equivalent manufactured by Schott.

They used picosecond pulses and reported that the nonlinear response was slower, in fact longer than the 10 ns pulse used Jain and Lind. This can be related to luminescence temporal behaviour which is globally slow for some materials and shows a slow component for others.

DFWM Study. The phase conjugated reflectivity measurements by Jain and Lind all fell in the saturation region. Conjugate signal intensity as a function of the laser intensity was studied in the unsaturated region and at the onset of saturation. This result was compared with saturation of absorption.

Interesting results were observed after studying the two glasses Corning 3-68 and Schott OG 530. These two glasses had the same cutoff point, i.e., 530 nm. The wavelength used was 532 nm. Corning 3-68 used was 3 mm thick with an optical density at 530 nm $=1$ ($\alpha L=2.3$, where α is the absorption coefficient and L is the thickness). For the optical phase conjugation and the luminescence a 5 mm thick OG 530 having optical density of 0.5 $\alpha L=1.15$ was used.

Nonlinear response time was measured for both these glasses by using four wave mixing techniques. The results were obtained using delay of backward pump. Schott OG 530 was seen to have an exponential decay with a time constant of 40 ns. In the case of the Corning 3-68 filter the curve can be decomposed as the sum of two exponentials, the faster one being weak with a time constant of 0.5 ns and the

slower one with a time constant of 11 ns. The authors note that since the largest delay used is only 3.8 ns, the accuracy of the long time constant is poor.

The main conclusion drawn from this study was that nonlinear response of these glasses was slow. Schott OG 530 showed a definite slow nonlinear response while Corning 3-68 had a weak fast component and a dominant slow component. However, there is evidence that there is considerable variation in different batches of the same Schott or Corning glasses.

Luminescence Studies. In the case of luminescence studies Corning 3-68 showed both a fast and a slow component. The fast component is tentatively attributed to the electron hole plasma recombination. The slow component is found to have a time constant of 40 ns.

For Schott OG 530 filter, the luminescence does not show any fast component. It clearly decays very slowly with a typical time constant of 400 ns. The luminescence quantum yield is much larger for the Schott glass than the Corning.

The authors attribute the slow component to luminescence from the impurity levels. The different behaviour of Corning 3-68 and Schott OG 530 is due to different nature of impurity in them.

Saturation of DFWM and Absorption. The threshold levels for absorption saturation and saturation in optical phase conjugation are quite comparable. Onset of saturation of absorption and optical phase conjugation occurs at 1 mJ/cm^2 for Corning 3-68 glass and ~ 7 mJ/cm^2 for OG 530 filter.

2.3.3 Aging in Semiconductor Doped Glasses

Aging effects have been discussed in detail by P. Roussignol et al. [22]. They discuss light induced darkening effect and formation of permanent grating in these

glasses. The two effects are related, almost certainly the permanent gratings being caused by alternate bands of darkened and undarkened glass. They also believe aging effects to be the reason why experimenters have often arrived at contradictory results.

Experiments were mainly performed on OG570 using a tunable dye laser providing pulses of 10 ns duration with a wavelength tunable in the 560-595 nm range. For fluences lower than $\simeq 0.5$ mJ/cm^2 the conjugate signal remains a constant but for larger incident energy, the conjugate signal decreases as a function of time. Typically for an incident fluence of $\simeq 5$ mJ/cm^2, it drops by a factor of 2 in about 10 min corresponding to 3000 laser shots. The larger the incident flux, the shorter is the time constant of this decrease. The conjugate signal does not drop to zero, however, it decreases by a factor of the order of 10 and then remains constant.

Holographic gratings of some sort of permanent nature have been observed to form. In an experiment OG 570 glass is exposed for a few minutes to only two beams, the forward and the probe. If we then send the backward-pump beam alone, even hours or days later, we still get a diffracted beam. This is similar to a photorefractive effect. The writing speed of the of the grating increases with incident energy fluence. The gratings can be erased by shining a single beam onto the glass. The time constant for erasure decreases when the erasing beam intensity increases.

The rate is roughly proportional to the incident fluence, with the existance of a plausible fluence threshold that could explain why these gratings are not erased by daylight. The writing and erasing process cannot be repeated in these glasses. After one cycle one always ends up with a darkened material and the permanent grating is no longer possible.

The darkening of these glasses is permanent at room temperature but is not irreversible. When such a darkened glass is heated to 450 °C for a few hours it

recovers its original appearance.

2.3.4 Effect of Aging on Glass Properties

Phase Conjugation. Darkening of glass decreases its efficiency as a phase conjugating medium. When we compare a fresh sample of OG530 and a darkened one, working at low intensity, the normalized conjugate signal decreases by a factor of 100 when 10 ns pulses are used and by a factor of 15 when 28 psec pulses are used.

Permanent gratings are formed without any observable darkening but the authors feel that permanent gratings and darkening are caused by the same photochemical mechanism.

Luminescence Spectra and Temporal Behaviour. Luminescence spectra were obtained by shining a laser beam onto the sample collecting the luminescence from the same side to avoid reabsorption problems as much as possible, and detecting it with a monochromator - plus - photomultiplier tube system. The exciting source was cw Ar^+ laser at 488 nm. The luminescence is time integrated and is shown uncorrected for spectral response of the detection center. See Figure 8.

For the non darkened glass two features are observable, a fairly narrow peak at 557 nm and a very broad band peaking at around $\lambda=750$ nm. The narrow peak is due to interband recombinations: electrons at the bottom of the conduction band recombine with holes at the top of the valence band. The position of this narrow peak corresponds to the bandgap, and indeed we observe a good agreement between the value determined this way and absorption spectrum.

The authors believe the second broad peak to be due to trapped - carrier recombination. According to Warnock and Awschalom [28] this broadband is related to surface effects. Chestnoy et al. [29] assign it to multiphonon - induced trapped carrier recombination.
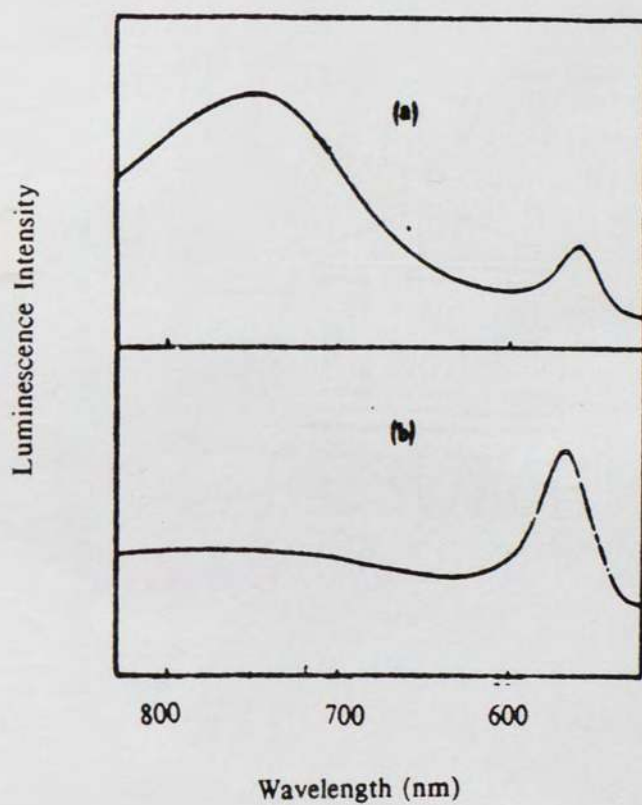
Figure 8. Luminescence spectra obtained with a cw Ar^+ laser for (a) a non darkened Schott OG 570 glass and (b) a darkened Schott OG 570 glass. For (b), the vertical scale has been expanded ≃5 times Ref. [22].

If the above measurement is repeated for the same glass (OG 570) after darkening, the narrow peak (somewhat weaker) is still observed, but the broad band has almost completely disappeared.

This may be because the trapping centers are no longer available. The overall quantum yield is drastically reduced.

2.3.5 Possible Theories for Darkening

Darkening is a photochemical effect. It could be similar to color center formation or the photochromic effect. It is probably due to carrier (electrons or holes) trapping on impurity or defect sites. In these semiconductor microcrystals impurity sites may be true impurities or surface states.

Light induced carriers get trapped on sites. Due to carriers getting trapped, the trapping sites are no longer available leading to slow decay as well as efficiency of these materials.

It is also worth mentioning that formation of permanent gratings and the darkening effect are not due to thermal effect. The temperature rise that has been calculated for the semiconductor microcrystals is only a few degrees. Furthermore, the darkening disappears after a heat treatment, as stated earlier.

2.3.6 Role of Traps in Nonlinearity

Remillard and Steel [23] believe that large nonlinear response measured by them is due to the filling of deep level traps by the decay of the electron-hole excitation produced by the forward pump and probe.

Experiment. The authors performed DFWM and nearly degenerate four wave mixing (NDFWM) experiments on Schott optical filter OG 590 which is doped with CdS_{1-x}
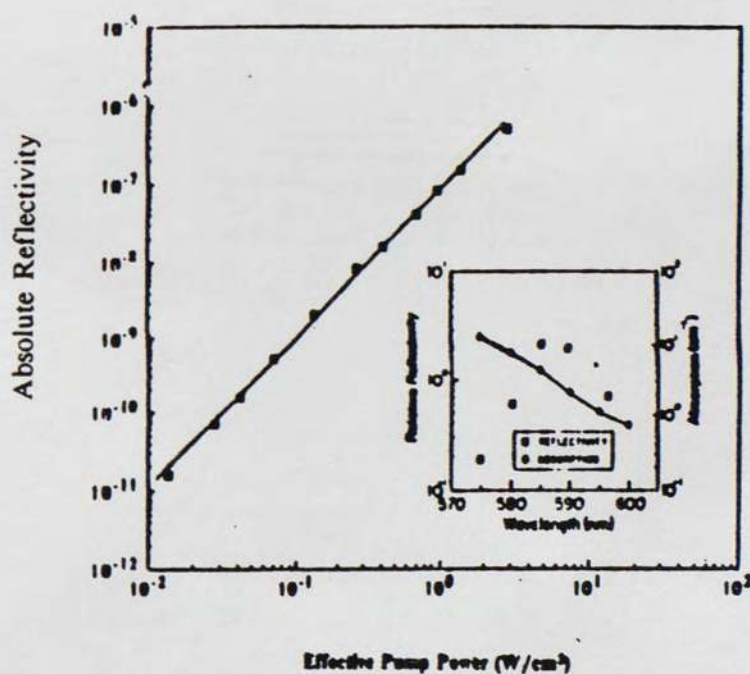
Figure 9. The FWM reflectivity measured as a function as a function
of pump intensity. The straight line has a logarithmic slope of 2. The
inset shows DWFM reflectivity as a function of wavelength at a constant
pump intensity. The open points represent the absorption spectrum of the filter. Ref.
[23].

Se$_x$ where x is estimated to be 0.2. In these experiments the probe frequency could be varied by using method of cross-correlated optical fields for measurement of bandwidths small compared with the laser jitter. The experiments were done at low pump intensities and phase sensitive detection was used to perform the measurements. Usually the forward pump beam was chopped.

First optical phase-conjugate reflectivity (defined as the ratio of the signal power to incident probe power) as a function of the pump power. Figure 9 shows the data taken at $\lambda=589$ nm where the nonlinear response was large. The solid line has n=2 as the slope. The nonlinear susceptibility χ^3 is estimated to be equal to 10^{-7} esu for L= 0.3 using the relationship:

$$R = \left[\left(\frac{2\pi\omega}{cn} \right) \chi^3 \right]^2 \left(\frac{8\pi}{cn} \right)^2 L^2 \, I_f \, I_b$$

Figure 9 inset shows a comparison of DFWM response and absorption coefficient as a function of wavelength. As expected, the nonlinear response decreases at short wavelength owing to an increase in the pump absorption.

The grating relaxation rate was measured by measuring the NDFWM relaxation rate using the method of cross-correlated optical fields. Low intensity (<500 mW/cm^2 was used. FWHM linewidth of 4400 KHz was measured linewidth was found to be indipendent of intensity (<5 W/cm^2) and the angle between pump and probe.

In their measurements nonlinear response was found to be independent of backward pump detuning as the laser was tuned into the red. As the backward pump laser was tuned into the green the nonlinear response began to decrease owing to absorption of the backward pump.

Conclusion. In the experiment the forward pump and probe are copolarized and the backward pump is cross-polarized. The production of the electron-hole pair is

proportional to the product of the field amplitudes (E_f , $E_p{}^*$ + cc.) resulting in a spatial modulation associated with the pair.

As a result of the decay to the traps, the filled traps are also spatially modulated. The signal results from a scattering of the backward pump off the resultant absorption and dispersion grating produced by the spatially modulated traps.

The long grating relaxation times (72 μsec) suggest that trap lifetimes are considerably longer than earlier results. The authors suggest two possible reasons, the first is that on the time scale of the earlier measurements, the traps did not have time to fill up. That is to say, the decay time from the conduction band to the traps is long compared with the measurement times. The other possibility is that when high power pulse lasers are used, the traps completely fill saturating this part of the nonlinear response.

Temperature effects on relaxation times were measured. As we cool the material, the linewidth reduces considerably implying an increased trap life time. This suggests that trap lifetime is determined by a phonon mediated process and lower temperature causes a reduced phonon-induced relaxation.

The authors believe that these traps are associated with the glass-semiconductor interface due to their long lifetimes.

2.3.7 Solarization in Glass (BK-7)

Solarization characteristics were measured Henesian and Weber [24] in BK-7 glass at 532 nm. They used a technique involving pulsed photo induced thermal lensing of a continuous wave probe beam. This is because of the very sensitive nature of the measurements performed. They derive 532 nm by frequency doubling a Nd:Yag laser at 10 Hz. The probe is at 632 nm derived from a high stability Helium-Neon laser "probe " laser. Their experimental set-up was quite complicated and they obtained important data.

Data

Figure 10 illustrates the induced linear absorption coefficient α (cm^{-1}) at four pump fluence levels (ranging from 9.3 to 22.9 J/cm^2) versus the number of shots into the laser. It can be observed that the solarization level rose slowly with the number of laser shots and then saturated.

Figure 11 plots the absorption coefficient from previous figure at fixed no. of laser shots vs the input J/cm^2. For $> 10^3$ we observe a greater than linear dependence of induced absorption on input fluence (intensity). For 10^4 shots the solarization shows the effect of saturation as evident in Figure 11. A log-log plot of the data in Figure 12 indicates that the slope of the curves remain near n=2 even at as high as 1.6×10^4 laser shots. Only the lowest curve at 100 laser shots with a slope of n=0.97 shows appreciable deviation from quadratic behaviour.

Possible Reasons for Solarization

The authors believe the solarization mechanism to be like a color center formation process involving electron trap sites above the valence states caused by the imperfections in the glass. The uv absorption edge (3.7 eV) of BK-7 at 340~350 nm (α=0.1 cm^{-1}) is well within the photon energy (4.7 eV) of the 2ω light and electron-hole pairs may be generated which subsequently fill the trap sites.

The saturation characteristic is probably due to the finite number of absorbing color- centers that can be formed in the irradiated volume.

The authors conclude that quadratic dependence of solarization on laser intensity is indicative of a two photon - induced color center formation process.

SOLARIZATION DATA RUNS

?BK7009.FIX = 22.3618J/CM^2, 3.78969E+09W/CM^2
?EK7010.FIX = 19.2401J/CM^2, 3.18934E+09W/CM^2
?BK7011.SMT = 12.6759J/CM^2, 2.10121E+09W/CM^2
?BK7012.FIX = 9.33713J/CM^2, 1.54777E+09W/CM^2
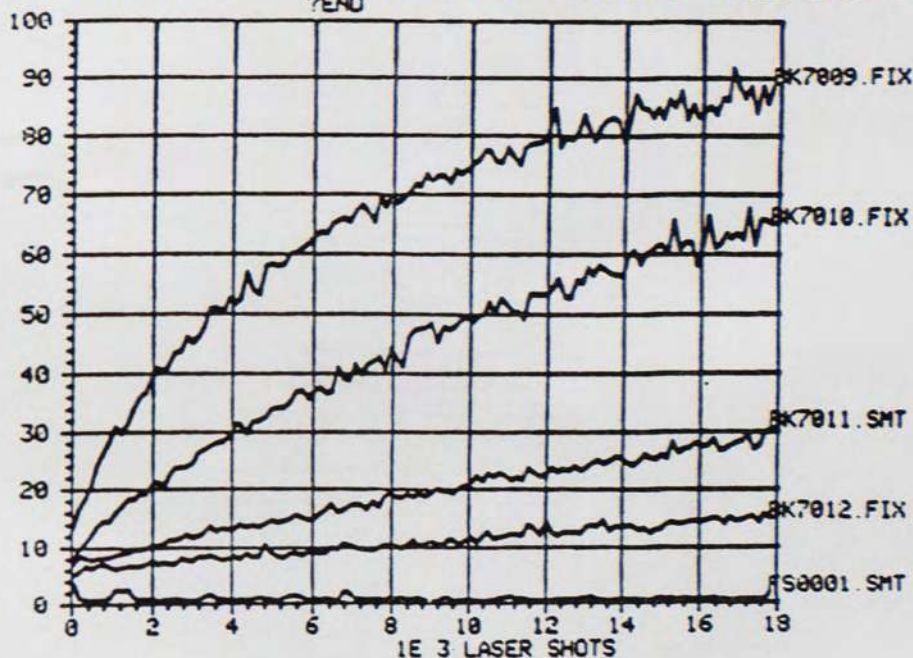?FS0001.SMT = 24.4463J/CM^2, 4.05234E+09W/CM^2
?END

1E-3 ALPHAX(CM^-1)

Figure 10. Linear absorption coefficient as a function of number of
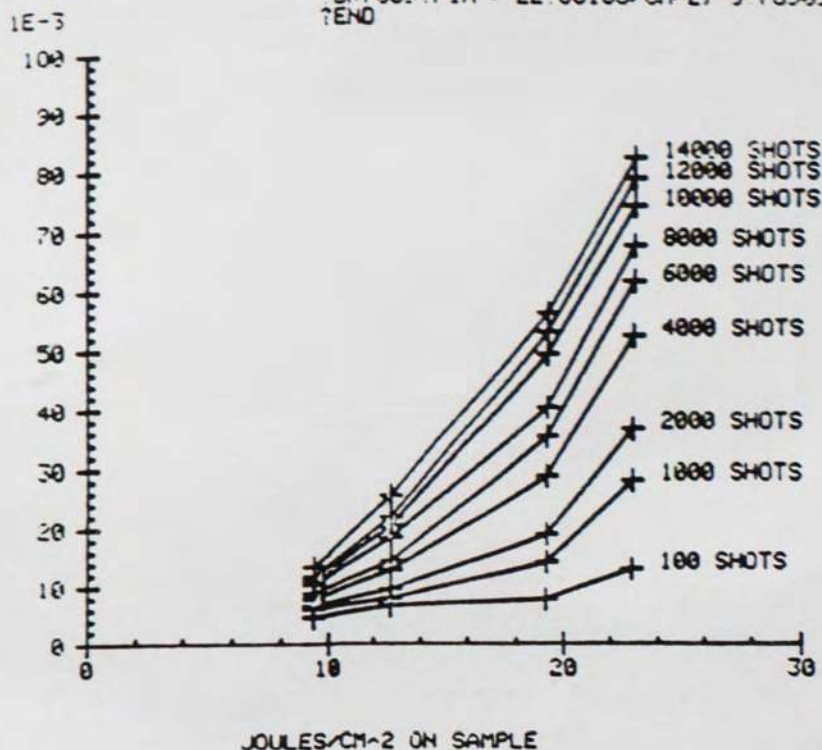laser shots for four different fluence levels. Ref. [24].

Figure 11.The absorption coefficient from previous figure at fixed number of laser shots as a function of the input fluence. Ref. [24].

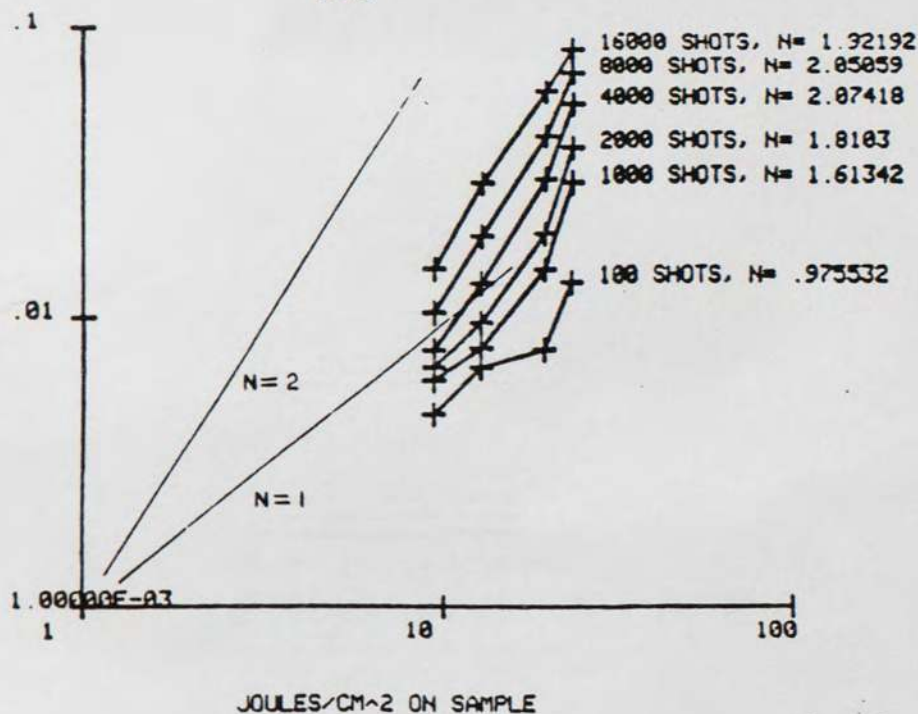Figure 12. Log-Log plot of Figure 11.

CHAPTER 3

EXPERIMENT

3.1 Motivation for Experimentation

After the literature review several doubts arise regarding the true nature of traps in the microcrystallites and the reason behind darkening.It is also useful to characterize the darkening. Darkening could be attributed to a color center effect. According to Ruossignol et al. [22] these color centers could be impurity or defect sites and the electrons were getting trapped permanently. But then they also believe that these sites also act as recombination centers, this is confusing, because then these sites should not hold electrons permanently. In studies done on cubic zirconia by Mansour et al. [30] color centers were created at high intensity by two photon absorption. The color in the material was bleached when it was irradiated with low intensity 532 nm pulses. This was because little two photon absorption could occur at low intensity and no more carriers could be trapped at the color centers. However, carriers at defect sites (color centers) get excited to a higher energy state using single photon absorption and relax back to the ground state thus leading to loss of color. The color got bleached when the material was left standing at room temperature for a couple of days. In the case of glasses, however, darkening could be removed by heat treatment at 450 °C. The similarity of the phenomena suggests that a similar kind of mechanism might be occurring in the semiconductor doped glasses. The following reasons were the motivation behind the experiments.

1. To establish the suggested threshold nature of darkening.

2. How darkening evolves with time.

- 32 -

3. Whether it is intensity dependent or fluence dependent.

4. To propose models for the physical processes occuring during darkening and to determine whether darkening is a phenomena entirely restricted to the base glass or only the microcrystallites or both.

3.2 Experimental Arrangement

3.2.1 Basic Schematic

The basic experiment set up schematic is shown in Figure 13. The Nd YAG laser produced pulses of picosecond duration at 1.064 micron wavelength. The basic repitition rate of the laser was 10 Hz.

The output from the Nd YAG laser was frequency doubled using a second harmonic generator. The resulting laser pulse was green in color (532 nm). A 1 m focal length converging lens was used around 55 cm in front of the sample plane to focus the beam. The HW1/e^2 M measured in vertical direction was 457 μm and in horizontal direction was 395 μm. See Figure 15.

A HeNe laser beam is used as a probe to measure transmission at 632.8 nm. The HeNe beam is chopped and then a tight focus is produced using a lens with focal length equal to 40 cm. The HW1/e^2 M of this red light is measured to be 83 μm. See Figure 14. A microscopic glass slide is used as a beam splitter for the HeNe laser so that the input to the sample can be measured. The input and output detectors have red spike filters to eliminate noise due to stray light sources. Appropriate neutral density filters are used so that output voltages of both the output and input detectors are very similar.

The output from the detectors is fed to the phase sensitive detector. The PSD is selected to measure the difference of the two signals at its input terminals. The difference signal of output and input detector is measured and is given as a D.C. level at its output terminal. The output is sampled every 0.1 second by the computer.

Figure 13. The basic experimental set-up.

As the glass is irradiated, it darkens and output minus input detector signal decreases.

3.2.2 Equipment Used

1. Nd-YAG Laser, 10 Hz, Q switched mode locked and a variable pulsewidth.

2. Second Harmonic Generator: M/N 53-122, manufactured by INRAD

3. Helium Neon Laser: 15mw maximum output, manufactured by Melles Griot

4. Chopper motor speed controller: Model 3828, manufactured by Ithaco

5. Chopper motor: model 382A, manufactured by Ithaco

6. Phase sensitive detector: model 353, manufactured by Ithaco

7. Detectors: large area photodiode with rise time of microseconds,

    associated circuitry includes an A/D converter

8. Energy detectors:

a. Model RKP-312, 183.5 V/J, manufactured by Laser Precision Corp.

b. Model ED 200, 10.09 V/J, manufactured by Gentec.

9. Spike filters

10. Neutral density filters

11. XYZ movement holder, manufactured by NRC

3.2.3 The Data Acquisition System

This system consists of a IBM clone which is interfaced to the detectors and stepper motor via an interface device. This device is called a converter box. It has 12 possible connections for the detectors. The negative going signals are recieved from the detectors by the converter box. The converter is responsible for signal processing. It digitizes the data and feeds it to the computer. The first connection is with a detector that takes its light input from the oscillator of the laser. This triggers the system and the voltages at the other connections are sampled by the box in rapid

succession. All this data is digitized by this converter box and is fed to the computer.

The converter box also has an interface circuitry for the stepper motor. The stepper motor is used for beam width measurement in our case.

3.2.4 Phase Sensitive Detector

A phase sensitve detector (PSD) was used to perform measurements. The probe beam was chopped at a rate of 1200 Hz. The number of slots was 40 and the chopper blade rotation speed was 30 rps.

The PSD is used to enhance the low signal to noise ratios. It is used as a cross correlator. The reference signal is derived from a photo-electric module consisting of a light-emitting diode and a photo-transistor. It is converted into a square wave and fed to the PSD. The PSD unit has a phase shifter to control the phase between the signal and the reference. The PSD rejects signals that are at a different frequency than the reference signal. It also rejects signals in quadrature with the reference. This enables us to achieve enhancement in signal to noise ratio.

The HeNe laser has a 2% fluctuation at its output as indicated in the specifications. In addition we can expect noise arising from the electronics of the PSD. Since our signal was not a rapidly varying one, a one second time constant at the averager was found to be appropriate. The PSD output was selected to give the difference between voltages at its input terminals A and B. We use appropriately scaled signals from output and input probe detectors at A and B respectively. Suppose if we just measured the output detector signal it would be hard to extract useful information from it due to noise problems. We expect a $\simeq 5\%$ reduction in the output detector signal due to darkening of the sample. However the noise present is of the same order. Hence, if we scale the signals from the output and input detectors such that the output is 10% higher than the input, then a reduction of 5% in the

output will actually cause a reduction of 50% in the net signal, i.e., (output - input). This signal can be easily observed with the noise in tolerable limits. Besides the advantage of using this is that both, the output and input detector signals carry the $\simeq$2% noise due to fluctuations in HeNe laser, hence their difference signal also has the same $\simeq$2% noise which is within tolerable limits. Nevertheless the best solution to this would have been to be able to ratio the outputs of the input and output detector or by having two lock-ins and ratioing by the computer. Unfortunately, the available lock-in amplifier could not perform a ratioing function and a second lock-in was also not available.

The phase shift is so chosen that signals are negative since the converter box is designed to receive negative signals.

3.2.5 Preliminary Alignment and Calibration

Beam Diameter Measurement. Beam scans of both the irradiating beam (532 nm) as well as the probe beam were done. The xy movement stand was connected to a stepper motor. A detector with a 50 μm pinhole as its window was placed on its stand. This was used to scan across the beam in both x and y direction. The beam scan measurements are shown in the Figures 14 and 15. HW1/e² M of probe beam was measured to be 83 μm in both vertical and horizontal axis. It should be noted that due to comparable dimensions of the pinhole and the beam diameter, our beam scans would show a larger beam width than the true beam width (the result is a convolution of a Rectangular function and a Gaussian function rather than a convolution of a Delta function and a Gaussian). HW1/e² M of pump beam (Nd:YAG) was measured to be 457 μm in vertical and 395 μm in horizontal axis.

Energy Calibration. A precalibrated energy detector or Joulemeter was used to calibrate a detector which was connected to the computer for energy measurement.
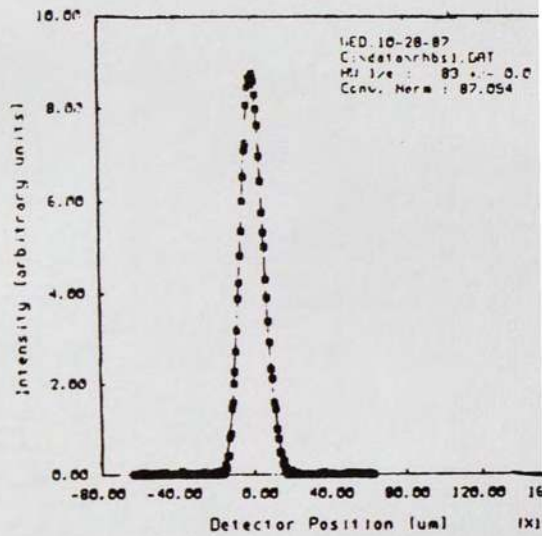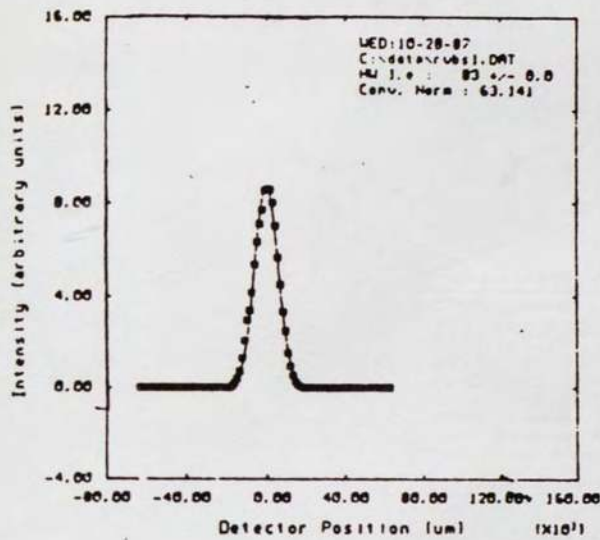
- 38 -

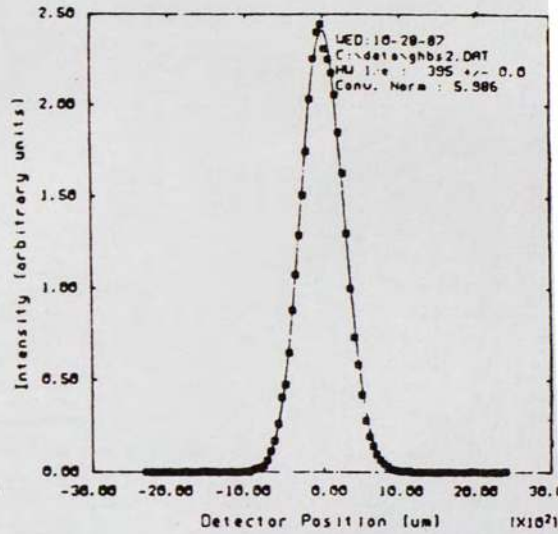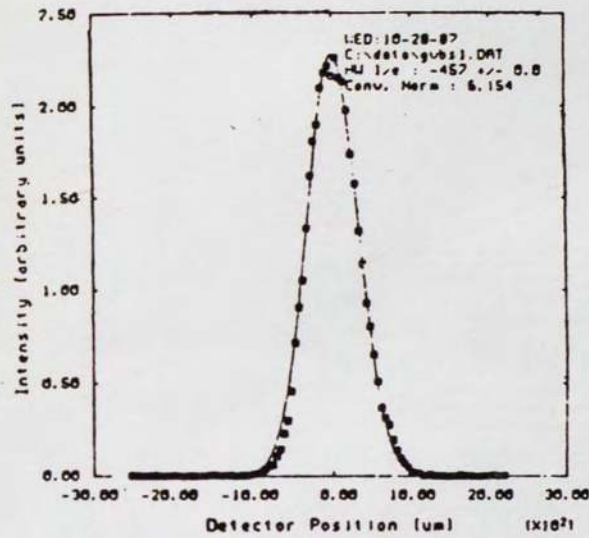Figure 14. Beam scan of the probe beam (HeNe laser). (a) vertical, (b) horizontal.

Figure 15. Beam scan of the pump beam (Nd-Yag laser). (a)vertical, (b) horizontal.

This energy detector was connected to the oscilloscope.

The laser was made to operate at 1 Hz. Readings were taken by computer and oscilloscope. A graph was plotted between the two readings. A line of best fit was drawn and a calibration constant of 367 µJ/V was calculated for the detector.

3.4 Results and Data

3.4.1 Introduction

The darkening caused by continuous irradiation of the glass by the laser was very small and could be barely seen. It was observed more clearly by placing the glass against a piece of white paper and looking from top.

An attempt was also made to see darkening effect using spectrophotometer over the entire spectrum. Nothing conclusive could be observed probably due to difficulties with using small sample areas or probably due to limited sensitivity of the equipment.

Transmission was measured at 632.8 nm for both clear and dark areas. The PSD was used with only the output detector connected. Measurements were made of HeNe beam incident on the output detector. The first reading was taken without any sample. Next reading was taken with a clear area of the sample in the path of the HeNe beam. The final reading was done with a darkened area carefully put in the path of the HeNe beam. This was accomplished by the sample holder which could be moved in x,y axis by the help of micrometer screws.

output detector reading

(without any sample)   =   100 mV

output detector reading

(clear area of sample)   =   88 mV

output detector reading

(dark area of sample)   =   83 mV

Transmission (clear area)   =   88%

Transmission (dark area)   =   83%

3.4.2 Darkening vs. Irradiation time

In this experiment the PSD was set at output minus input choice (A-B). This value was sampled by the computer. At an average fluence of 44.7 mJ/cm² and pulsewidth of 30 ps 4800 shots were allowed to irradiate the laser. The laser was operated at 10 Hz through out, except when repetition rate dependence was being studied. It can be observed from Figure 16 that decrease in transmission occured more rapidly during initial part of the irradiation, later rate of change decreases till transmission almost levels off to constant to constant value. After this no further change was observed.

Due to constant change in laboratory conditions and due to slow drifts that occured in the measuring system, which lead to regular adjustment it was difficult to relate accurately the change in transmission to the transmission coefficient. Through out this section, we choose to show all our transmission measurements in arbitrary units. Approximately one unit (arbitrary units in all figures) corresponds to a change of 1% change in absolute transmission. The value of initial point or the zero point have no relavance and are arbitrarily chosen. We also cannot compare two different graphs. As mentioned earlier, initial transmission is 88% and can drop up to ≃6%

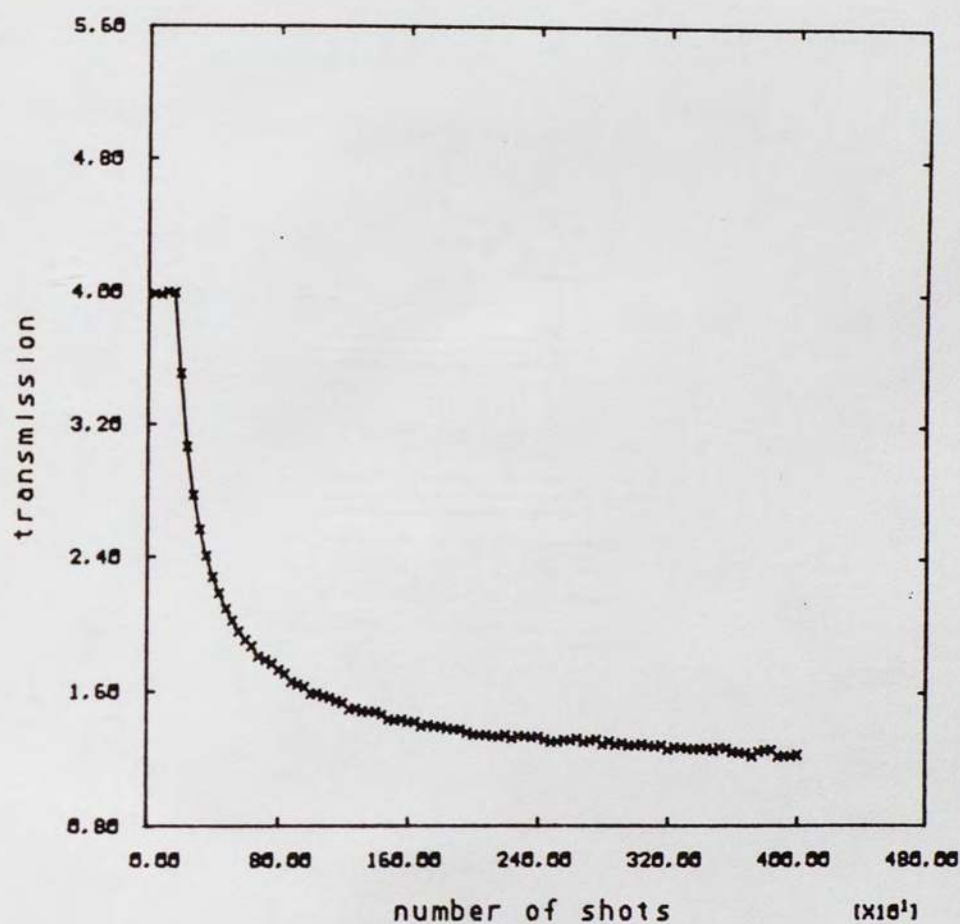Figure 16 . Transmission change (arbitrary units) for OG 515 irradiated at a fluence of 44.7 mJ/cm² for 4800 shots. The irradiating beam was blocked for the first 50 shots.

depending upon fluence and irradiation time.

3.4.3 Recovery

Another interesting fact was noted that when the laser was blocked, a slight recovery was observed. See Figure 17.

The recovery time was of the order of several seconds. It is indicative of some type of a slow mechanism. If irradiation is resumed after the recovery, darkening continues further and interestingly the slope (i.e. rate of change of darkening) is the same as it was just before the brief blockage time. See Figures 18 and 19. This could be the reason for the repetition rate dependence of darkening mentioned in the later sections.

The nature of time period of this recovery (i.e. several seconds) led us to believe that this was in some manner related to the material cooling off after experiencing a rise in temperature due to laser irradiation. To check on this an experiment was devised in which a second HeNe laser was used. This laser was set behind the sample and was brought to a tight focus at the irradiation point. This was to ensure that the sample continued to stay at the higher temperature due to the second HeNe lasser. All the three beams were made to overlap perfectly using the pinhole method of aligning. The pump beam was blocked after irradiating the sample for some time. Then the second HeNe beam is switched on. There was no enhancement or suppression of recovery noted. Therefore we could not be convinced that thermal reasons were indeed the cause of recovery in transmission .

3.4.4 Darkening vs. Fluence

Further experiments were conducted to see darkening changes as a function of fluence per shot. The pulsewidth was maintained at 30 ps for these set of experiments. The fluence per shot was controlled by changing the amplifier voltage
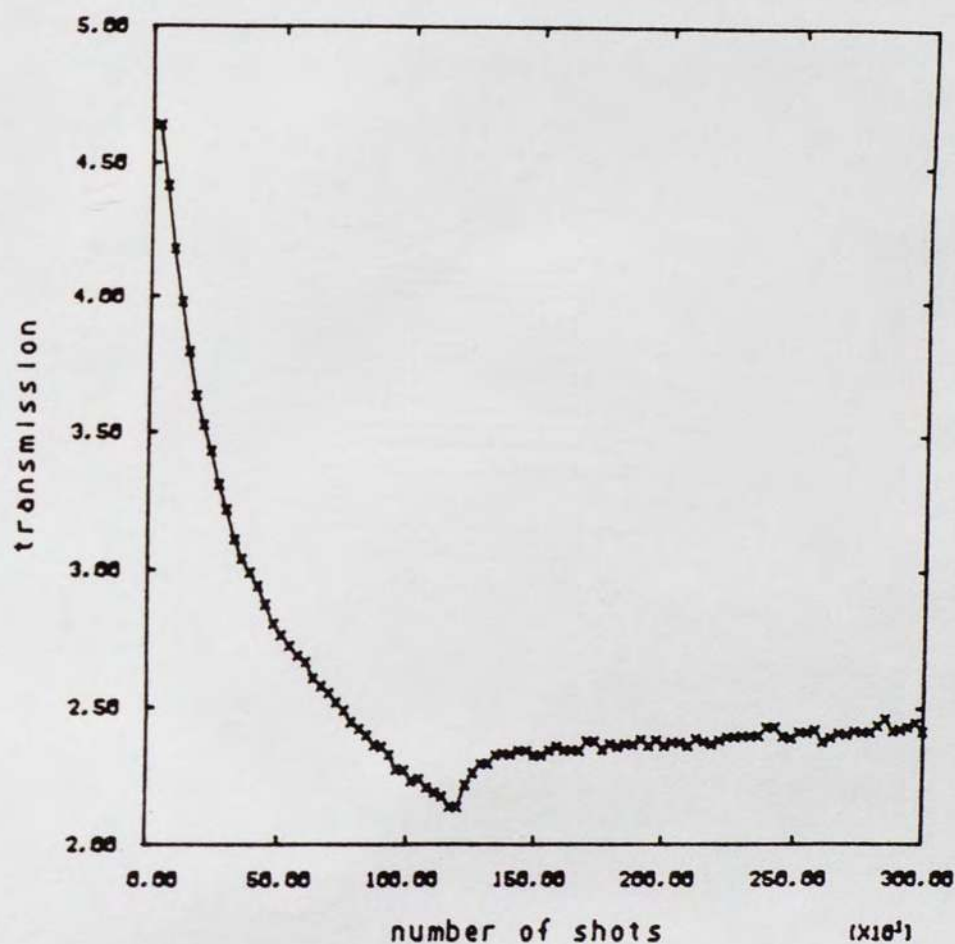
Figure 17. Transmission change (arbitrary units) for OG 515. It was irradiated at a fluence of 67.8 mJ/cm² for 1200 shots and then the irradiating beam was blocked.
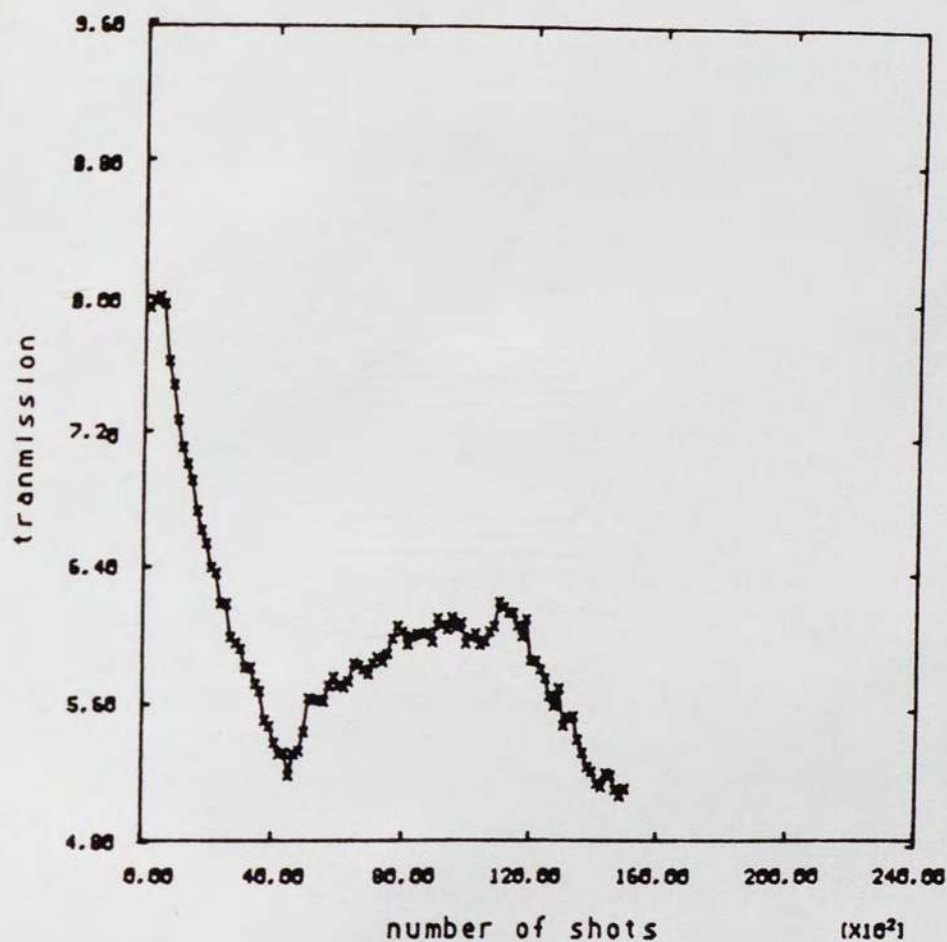
- 45 -

Figure 18. Transmission change (arbitrary units) for OG 515. Irradiating beam was blocked for first 600 shots and then resumed till 4500 shots. It was blocked again between 4500 to 12000 shots. Irradiation was resumed again from 12000 shots to 15000 shots. The irradiating beam fluence was 10 mJ/cm².
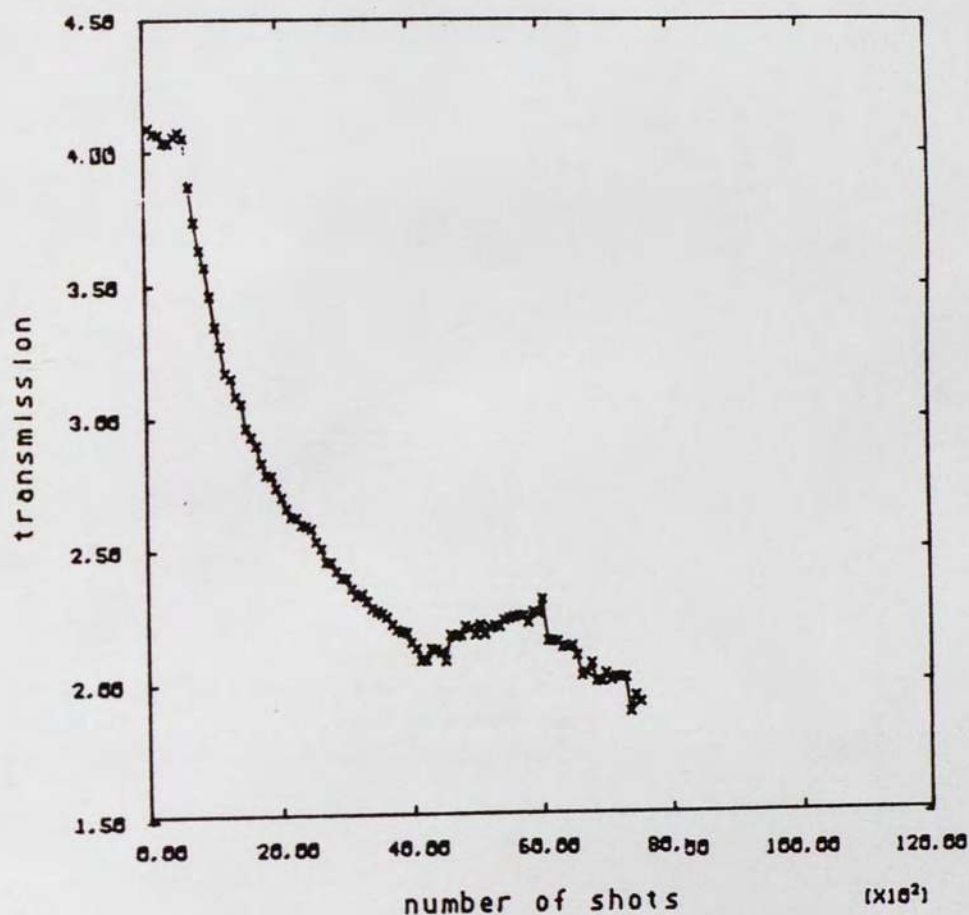
Figure 19. Transmission change (arbitrary units) for OG 515. Irradiating beam was blocked for first 300 shots and then was allowed to irradiate till 4000 shots. It is blocked again from 4000 to 6000 and then resumed again. The irradiating beam fluence was 12.7 mJ/cm².

of the laser.

As before it was observed that darkening occured rapidly and then levelled off. For a higher fluence per shot not only initial rate of increase was more but also the final saturation point was higher.

Experiments were done first at a lower energy per shot but over a larger number of shots. See Figure 20. The final darkening level or transmission coefficient almost levels of to a constant value. This constant level increased as higher fluence per shot was used.

At lower energy per shot very little transmission change was observed in spite of irradiating over a long period of time. This kind of behaviour suggests some kind of threshold, i.e., a certain number of carriers have to be excited at a time to achieve any darkening. This would also explain why no darkening was observed by just leaving the sample in ordinary daylight, because ordinary daylight was below the threshold. This is like a two photon absorption process which is proportional to the square of intensity

In another set of data taken for a lesser number of shots but for a higher energy. A similar characteristic is observed. See Figure 21. Here the early part (i.e., where rapid change occurs) is seen. It can be clearly observed that with higher fluence per shot the rate of darkening increases.

It is interesting to see a graph of darkening versus the total integrated fluence recieved by the sample. Each curve corresponds to different fluence per shot. See Figure 22. This graph is obtained by multiplying the x axis by fluence per shot. The conclusion drawn are similar to previous ones. More darkening can be achieved by irradiating with a fixed total fluence at a faster rate and shorter time than at a lower rate for a longer time. Figure 23 shows a log-log plot of transmission change versus fluence at 1000 shots in Figure 21. The slope $\simeq 1.5$.
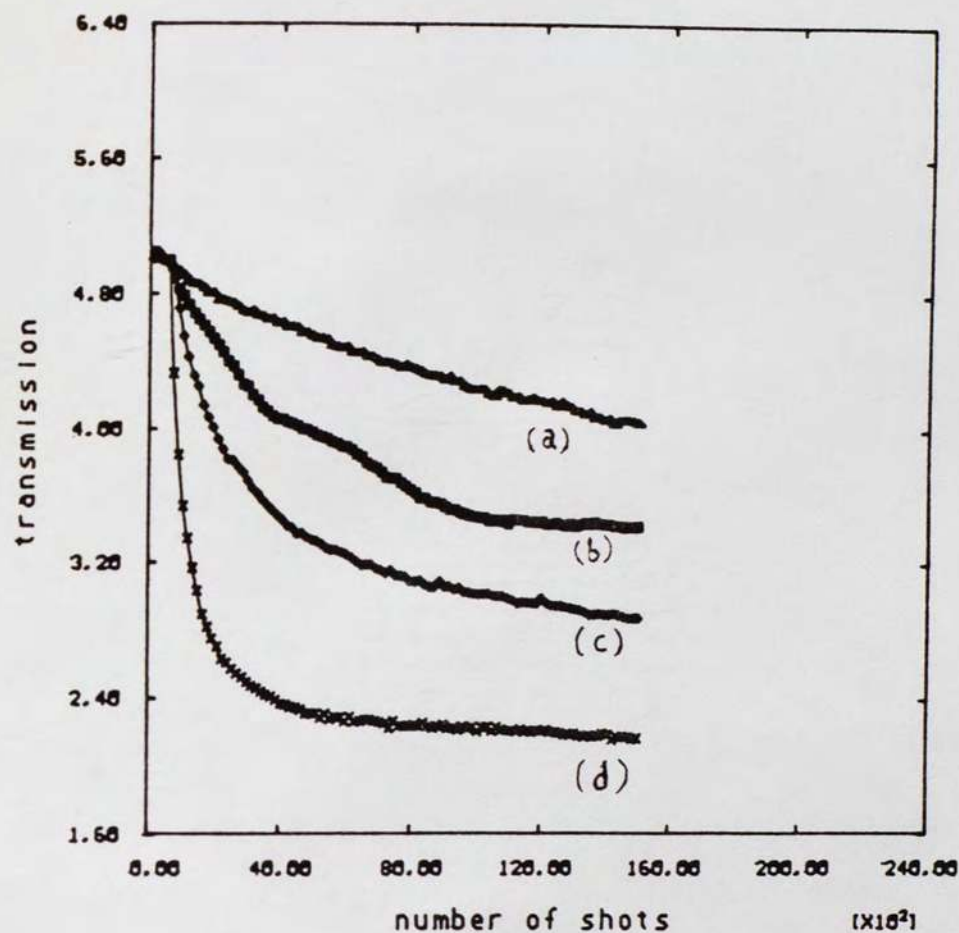
Figure 20. Transmission change for different fluences over 15000 shots.

Curve a - 3.9 mJ/cm²
Curve b - 5.2 mJ/cm²
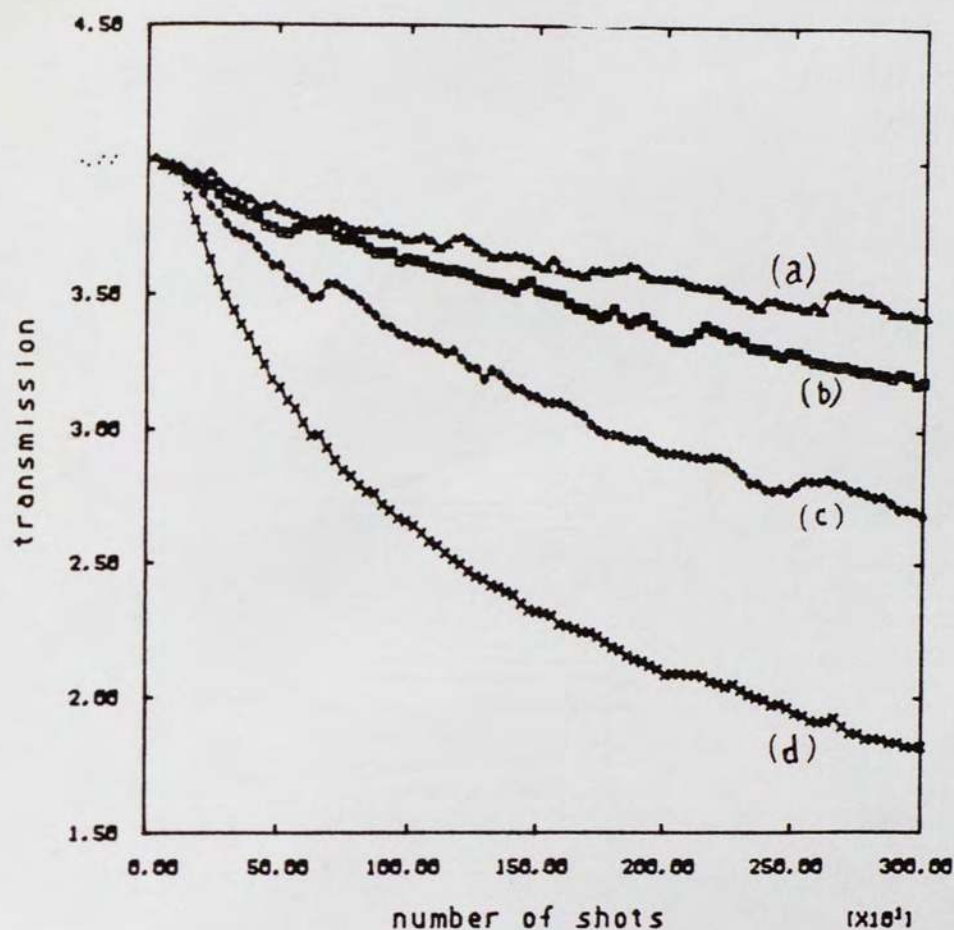Curve c - 12.3 mJ/cm²
Curve d - 31.2 mJ/cm²

Figure 21. Transmission change for different fluences over 3000 shots.

Curve a - 19.2 mJ/cm^2
Curve b - 21.2 mJ/cm^2
Curve c - 34.3 mJ/cm^2
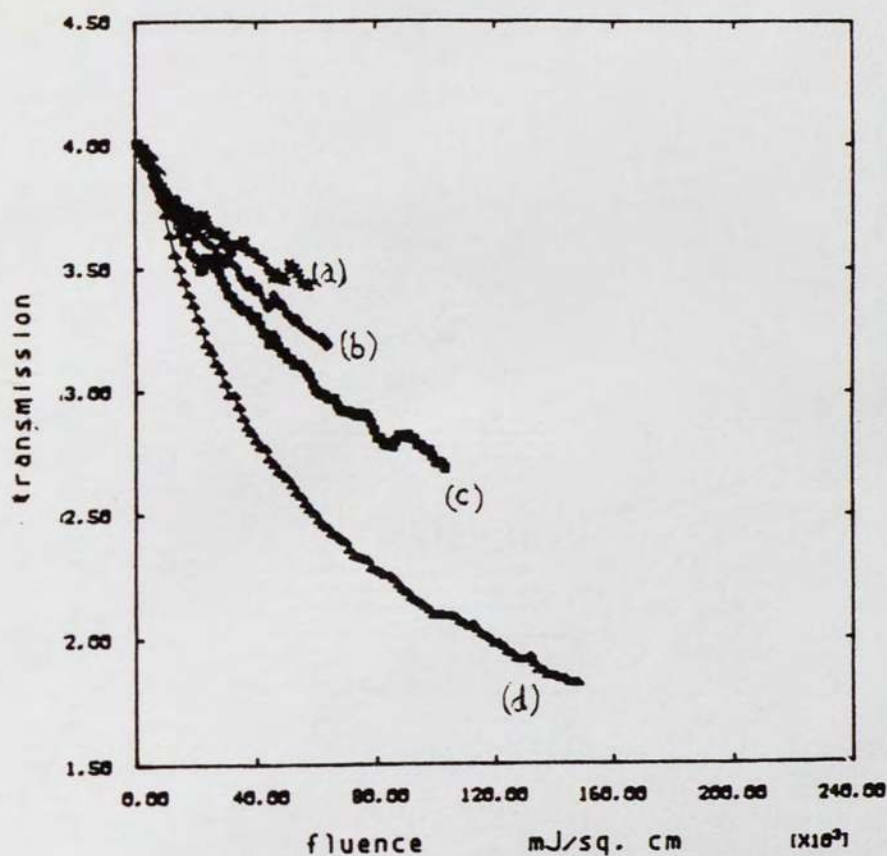Curve d - 49.2 mJ/cm^2

Figure 22. Transmission change as a function of net fluence irradiated into the sample for different fluence per shot. Obtained from Figure 21 by multiplying x axis by fluence per shot.
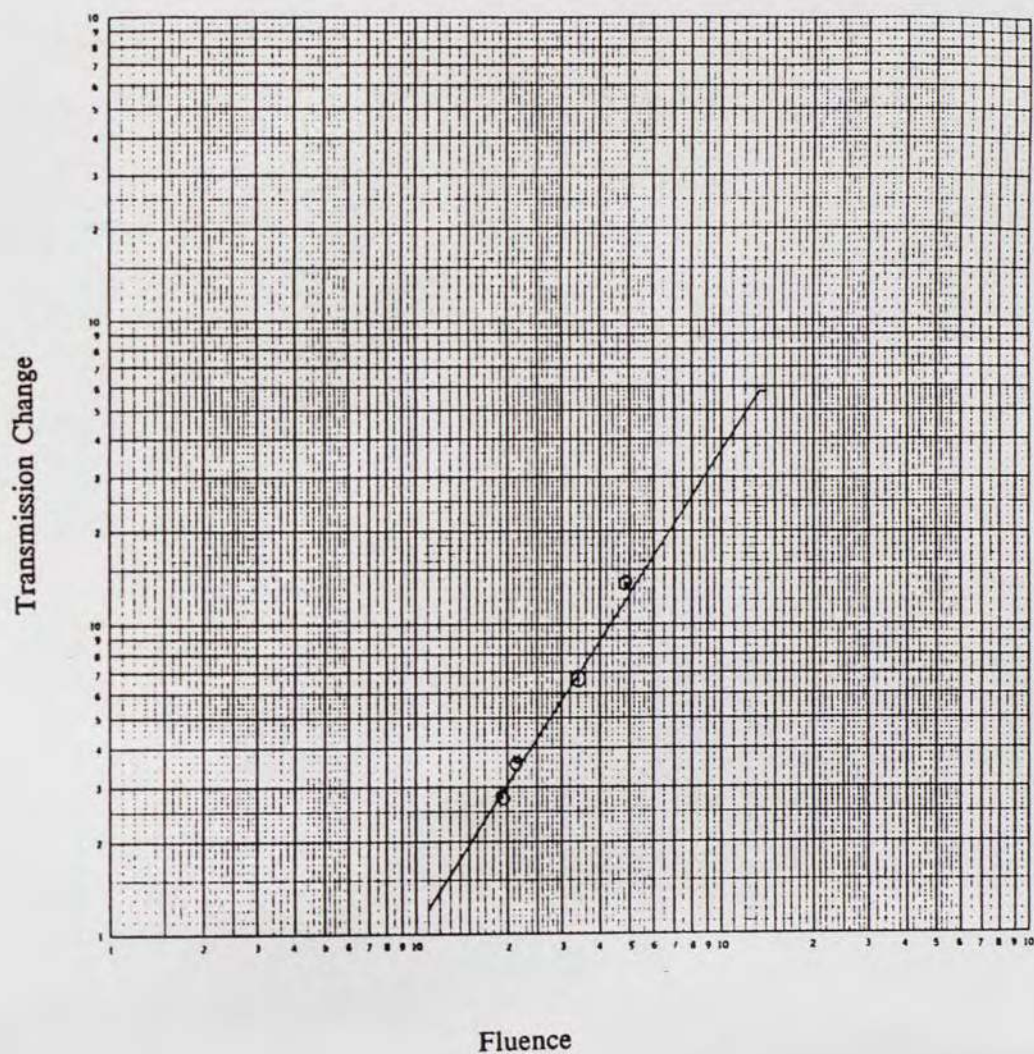
Figure 23. Log - log plot of Transmission Change vs
Fluence at 1000 shots in Figure 21.

3.4.5 Darkening vs. Repetition rate

Experiments were performed to see darkening as a function of repitition rate of the laser. Data were taken at repitition rate of 10 Hz, 5 Hz, 2.5 Hz and 2 Hz. It was not feasible to take data at lower repitition rate due to the extent of time involved. In general at lower repitition rate, darkening was slightly less than that at higher repetition rate. See Figure 24.

The reason could lie in the fact that there is some recovery in darkening as observed in previous experiments. At lower repetition rate, the time interval between two consecutive laser shots is more, therefore the glass has a greater time to recover between two shots. Suppose after the first shot there was time for some recovery in darkening, the second laser shot comes in and causes some darkening. Therefore the effective darkening due to these two laser shots is less than the sum of individual darkening by each laser shot.

3.4.6 Darkening vs. Pulsewidth

Experiments were conducted to measure darkening as a function of pulsewidth. With the fluence constant over a data set darkening was measured at different pulsewidths. See Figures 25 and 26. Pulsewidth can be changed by changing the etalon in the cavity for 30 ps, 100 ps and 200 ps pulsewidths. With a 30 ps etalon, an autocorrelation for a wavelength of 1.06 μm gave a HW1/eM of 28 ps. For 532 nm we estimate HW1/eM of 20 ps (less by a factor of square root of 2 due to frequency doubling). With a 100 ps etalon HW1/eM pulsewidth is determined from the ratio of the second harmonic energy to the square of the fundamental to be 64 ps and with a 200 ps etalon HW1/eM pulsewidth is estimated to be 140 ps (not calibrated).

It was observed that almost double the amount of darkening occured at 64 ps compared to 20 ps. At 140 ps darkening was quite close to that at 64 ps. At 64 ps
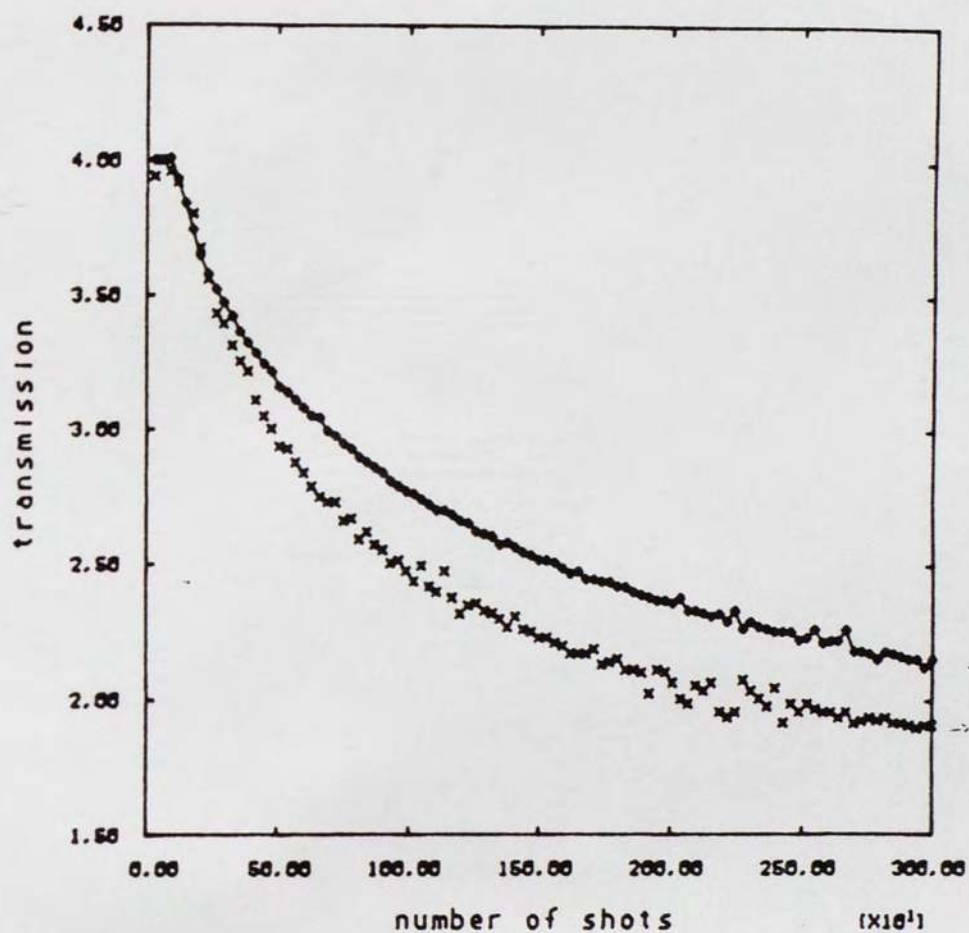
Figure 24. Transmission change for approximately same fluence but different repitition rate.
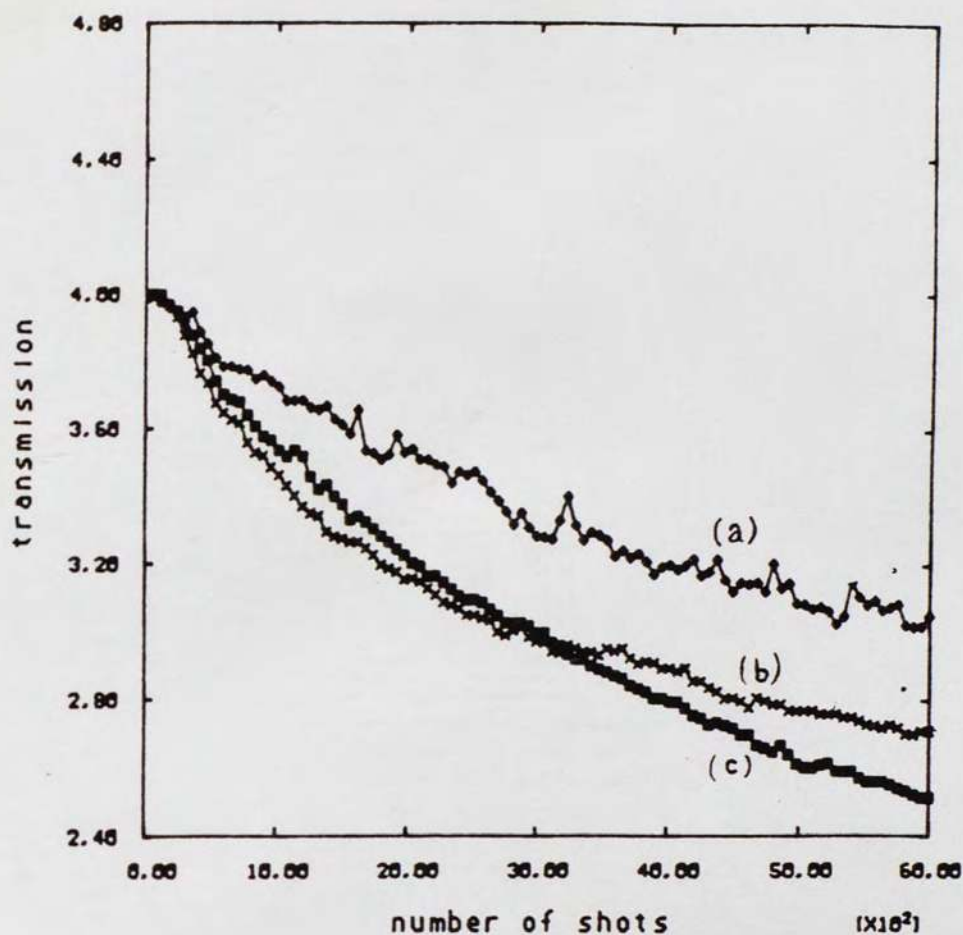
+ 28.9 mJ/cm² at 2 Hz
x 29.8 mJ/cm² at 10 Hz

Figure 25. Transmission change for different pulsewidths and approximately same fluence ($\simeq$ 14.1 mJ/cm^2).

Curve a - 20 ps
Curve b - 64 ps
Curve c - 140 ps

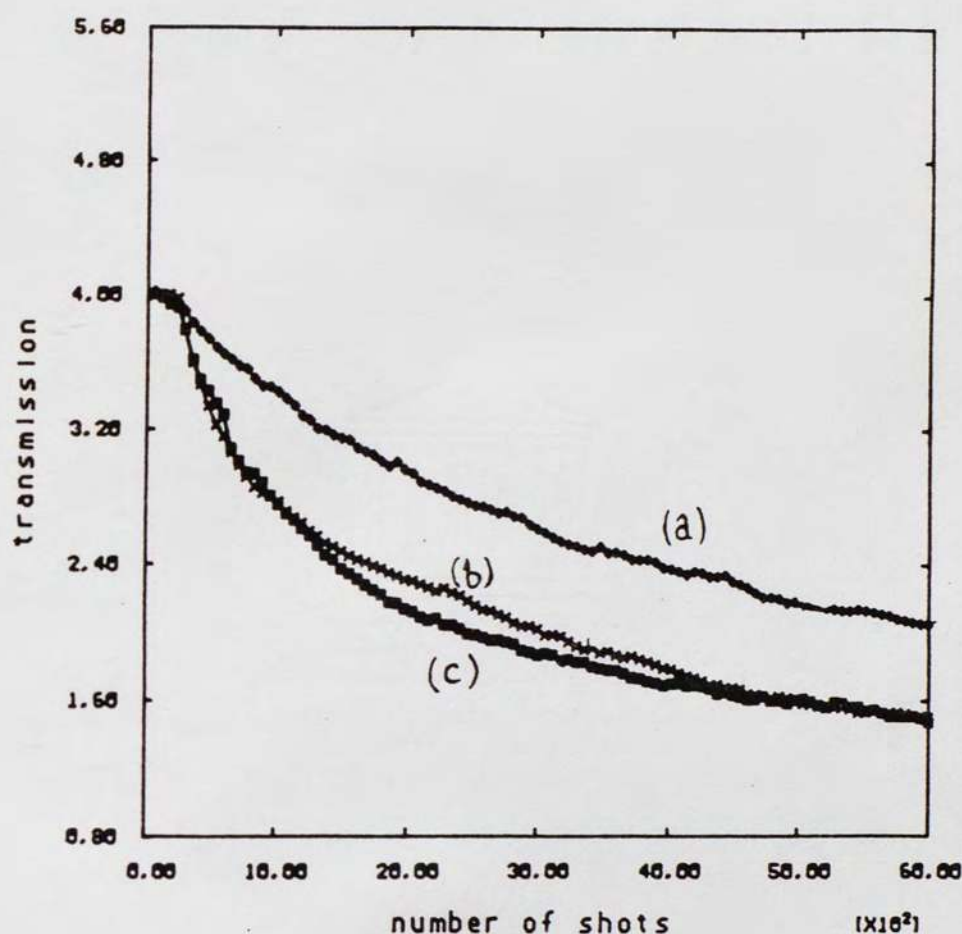Figure 26. Transmission change for different pulsewidths and approximately same fluence ($\simeq$ 24.6 mJ/cm^2).

Curve a - 20 ps
Curve b - 64 ps
Curve c - 140 ps

the intensity is less than one third yet it was twice as effective. Such behaviour could suggest several explanations. At 20 ps excitation of carriers that cause darkening might be getting saturated. Hence a fluence distribution over 64 ps might be more effective. There is also a possibility that absorption by a carrier occurs in two stages. This means that after the electron has been excited to a level it relaxes to get excited again to a new stage that causes darkening.

3.4.7 Darkening in Different Glasses

From the data taken it was observed that darkening occured in glasses with bandgap smaller as well as larger than the energy corresponding $\lambda=532$ nm. By and large Schott glasses incurred more darkening than the Corning glasses for a similar amount of irradiation.

In these experiments conducted (for comparison of different glasses) all irradiation was done at 200 ps for 5 mins at 10 Hz, i.e., 3000 shots total. It has been attempted to maintain constant fluence per shot for these data. Usually fluence per shot fluctuates significantly when examined from a shot to shot basis. In this experiments we measure the average value over the whole range.

The Schott samples we had had equal thicknesses and their initial transmissions (prior to irradiation) at 632.8 nm was equal or atleast quite close. On the other hand the Corning samples were more varied, with different thicknesses and different transmission at 632.8 nm.

It would be quite fair to make comparisons accurately of different extent of darkening in different samples of Schott glass. However for Corning, due to their different thicknesses it would be rather inaccurate to compare darkening. One can only get an approximate idea from the data presented.

TABLE 3

GLASS	FLUENCE (mJ/cm^2)	TRANSMISSION CHANGE (arbitrary units)
OG475	44.8	3.19
OG495	45.3	5.5
OG515	39.2	3.2
OG530	42.6	4.79
OG570	40.0	2.38
3-67	38.0	2.02
3-68	36.5	0.711
3-69	45.6	1.1
3-70	45.6	2.14
3-71	46.7	3.38

The darkening observed in different glasses had really no definite trend and no proper relationship between band gap and darkening could be noticed.

Figure 27 shows the extent of darkening in different Schott glasses and the manner in which darkening evolves with time. Figures 28 and 29 show darkening compared between equivalent Schott and Corning glasses.

It is therefore concluded that darkening is more likely to be related to parameters like size of the crystal, chemical composition of the base glass, impurity defects in the crystal, defect sites in glass etc. One major conclusion from this experiment was that mechanism of darkening is not related to the basic microcrystal since no dependence on band gap was seen. Glasses with larger band gap which should have allowed 532 nm to be completely transmitted also darken.
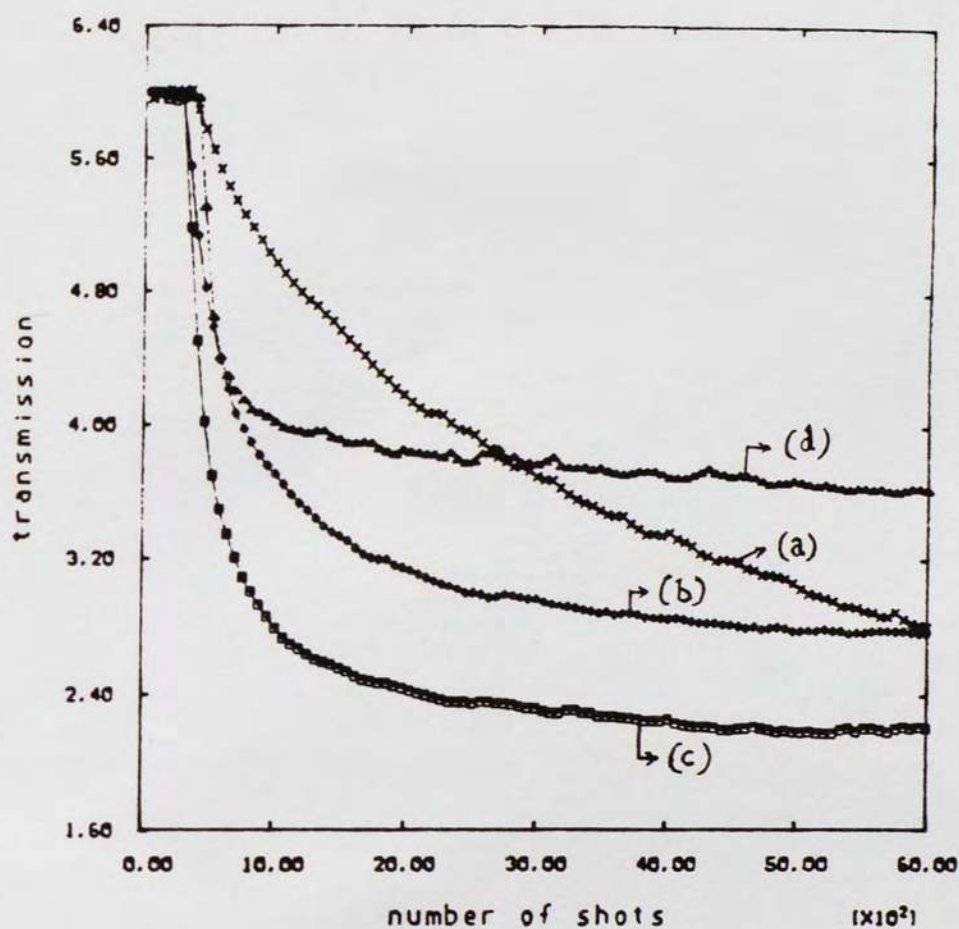
Figure 27. Comparison of darkening in different Schott glasses.

Curve a - OG 475
Curve b - OG 515
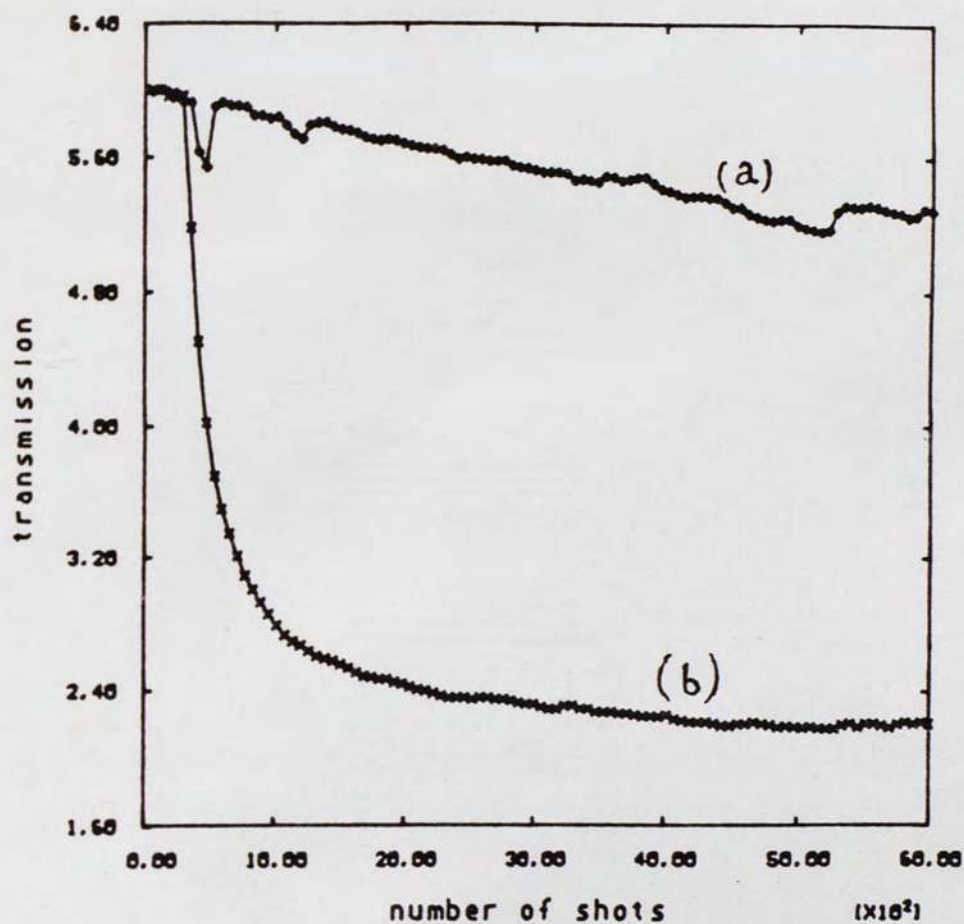Curve c - OG 530
Curve d - OG 570

Figure 28. Comparison of darkening in OG 530 and CS-3-68.

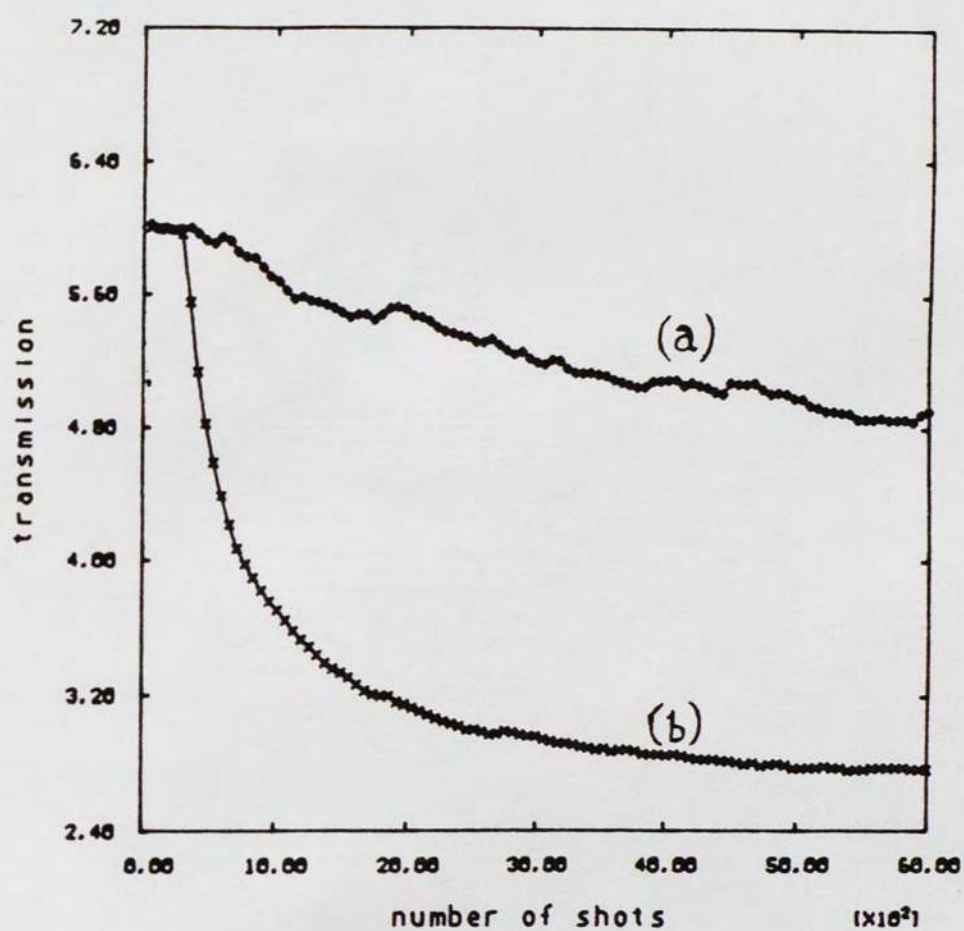Curve a - CS-3-68
Curve b - OG 530

Figure 29. Comparison of darkening in OG 515 and CS-3-69.

Curve a - CS-3-69
Curve b - OG 515

CHAPTER 4

CONCLUSION

With a substantial amount of information available from literature and our own experimental results we can attempt to understand the mechanisms that lead to aging effects. We have characterized darkening in great detail and can get some ideas about the mechanisms involved. In this final chapter we try to interpret our results and sum up information from the literature. We suggest possible mechanisms and the specific conclusions we derived from our study.

4.1 Discussion

The recombination mechanism of carriers in CdSSe microcrystallites consists of two paths, direct fast recombination and slow recombinations via traps. This has been agreed on by several experimenters. Several direct and indirect evidences for this have been studied like nonlinear response time and photoluminescence studies by Roussignol et al. [22], intensity dependent photoluminescence by Kwok et al. [31] etc.

The effects of aging have been identified by Roussignol et al. [22]. Aging leads to a lower nonlinear coefficient and a much faster nonlinear response time. It also leads to darkening. Mitsunga et al. [25] measured permanent changes in the relaxation time for light induced gratings (LIG) in Hoya R60 after different amount of exposure to laser irradiation. It was observed that as the sample was exposed to laser irradiation for longer times the relaxation time for the gratings began to decrease. Refer to figure 30. This was explained by the "removal of the trap levels"
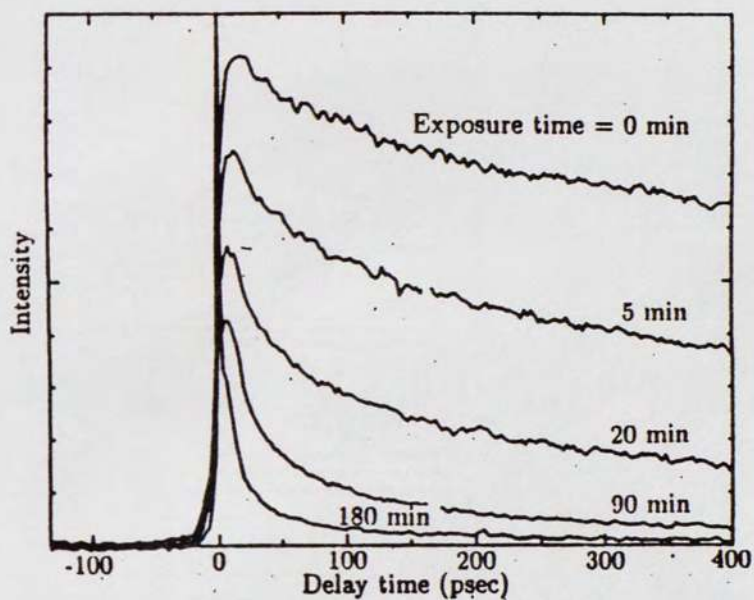
- 62 -

Figure 30. Signal intensity versus probe pulse delay for various
exposure time in the LIG measurement. 300 μm thick Hoya R60 sample
is used with wavelength = 613 nm. Ref [25]

due to laser irradiation which lead to a decrease in the number of carriers undergoing slow relaxation via these trap levels. However, there was no explanation offered as to how these trap levels were removed, they referred trap removal as an annealing effect by the laser. The authors did not notice any darkening accompanied with this phenomenon unlike Roussignol et al who observed both of the above phenomena in Schott OG 530. The fact that no darkening was observed by Mitsunga could be due to several reasons. The fluence values used by them were very small and the pulse width was also small (5 psec). Both of which lead to lesser darkening as we found in our experiments, even if large amount of laser shots were delivered as in the above case. Besides, transmission changes are usually small and 1%-2% transmission change can be barely observed by the naked eye or even measured accurately by a spectrophotometer. Therefore we cannot be sure to distinguish darkening and recombination center removal as two separate unrelated phenomena.

It is interesting to make qualitative comparison between time evolution of darkening we observed and the rate of removal of traps levels seen from experiments done by Mitsunga et al.[25]. Refer to figure 30 which shows light induced grating decay time measurements. There is a lot more change in the first 5 minutes than in the last 90 minutes. This implies that the trap level removal occurs more rapidly in the initial stages and then slows down as number of traps remaining also decrease. This is similar to darkening which occurs rapidly during the initial part of irradiation and then levels off.

Darkening also occurs in plain glasses. Solarization in BK-7 which is a borosilicate glass was studied by Henesian and Weber [24]. In their experiments much higher intensities were used ($\simeq 1.5$ GW/cm^2) with a larger number of shots delivered (18000) and a $\simeq 9\%$ drop in transmission was observed for a 1 cm thick sample. Pulsewidth used was 12 ns, therefore fluence per shot was $\simeq 10$ J/cm^2. Solarization was studied in different Schott glasses by Hagen and Snitzer [26] who observed

different solarization threshold for them. They observed the glasses to anneal at room temperature in 48 hours, but the solarization remained in the sample for weeks when kept at a temperature of -20 °C. Henesian and Weber did not observe any change in solarization after keeping the samples for a long period of time. Ruossignol et al. saw complete disappearance of darkening in semiconductor doped glasses after heat treatment at 450 °C. We saw small amount of recovery in transmission in OG 515 at room temperature over a few minutes, after which there was no further recovery.

Solarization is believed to be due to electrons being excited from valence states to trap sites which act like color centers. The trap sites are most likely due to imperfections in glass. Hence we can expect solarization characteristics to be related to the structural property and the chemical composition of the glass. The structure of the glass would depend upon the manufacturing methods. We have seen that drop in transmission is up to $\simeq 6\%$ in a 2mm OG515 sample as compared to a $\simeq 9\%$ drop in a 1cm BK-7 glass with high intensities for nanosecond duration in contrast to lower intensites for picosecond duration used on the semiconductor doped glasses. This implies that the microcrystallites enhance darkening. However, due to lack of knowledge about the chemistry of glass, microcrystallite and different darkening results obtained with the Corning sample we cannot be convinced that darkening and recombination center removal are the result of the same mechanism.

Our darkening results obtained with CS 3-68 and OG 530 are in fair agreement with photoluminescence studies done by Ruossignol et al. [22], if we believe darkening causes recombination center removal or vice versa. CS 3-68 darkens very little showing that it has very few recombination centers to be removed unlike OG 515 which darkens to a larger extent implying that it has larger number of recombination centers to be removed. In photoluminescence studies also we find that OG 530 has a larger quantum yield with vast majority of carriers undergoing slow recombination via centers. The CS 3-68 has a much lower quantum yield and

recombination occuring via both paths.

At this point we can identify two states, the trap sites and recombination centers. The trap sites are of more permanent nature that leads to darkening while recombination centers act as temporary intermediate levels for carriers undergoing slow recombination. Based on the above, we can suggest an explanation for the aging phenomena in semiconductor doped glasses. The electrons in the valence states are excited and get lodged at structural imperfectations, which we believe are present at the interface of the semiconductor microcrystallite and the glass. Filling up these trap sites inhibits the recombination center in the microcrystallite, which are probably the surface states. We are not sure whether the carriers that get trapped at these trap sites come from valence state in the glass or valence state in the microcrystallite. We however, have interesting results on how darkening is affected as pulsewidth is varied keeping the fluence a constant. We found that at 64 ps more darkening occured than at 20 ps and at 140 ps the darkening was quite close to that at 64 ps.

Figure 31 shows possible mechanisms that could lead to darkening. Given a certain fluence "two photon absorption" increases as pulsewidth is decreased while "two step absorption (without relaxation at intermediate level)" is not affected by change of pulsewidth within certain limits. Therefore the most likely mechanism is the two step absorption with a fast relaxation at intermediate levels. If the relaxation time from level a to level b was of the order of 20 ps, a pulsewidth of 64 ps would be more effective to excite a carrier at level b to go to level 2 which is the trap site. A 20 ps pw would not give sufficient time for a carrier to relax from a to b and then get excited again to go to level 2.

From the threshold nature of darkening we also know that sufficient number of carriers have to be excited to make the above mechanism possible. The trap sites were probably the reason for the semipermanent gratings observed by Ruossignol et al. [22]. The trap sites were filled, being spatially modulated by interference of
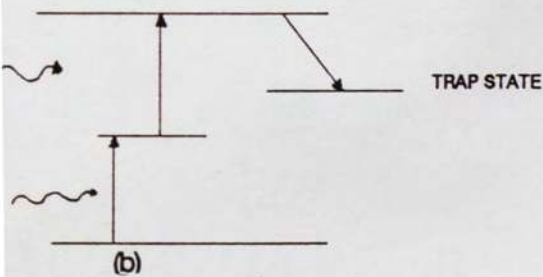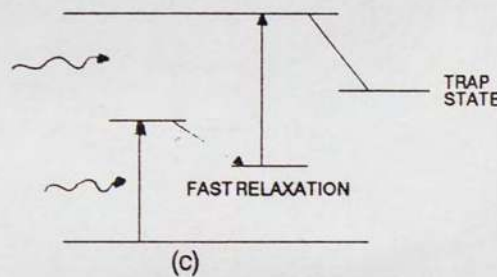
TWO PHOTON ABSORPTION

(a)
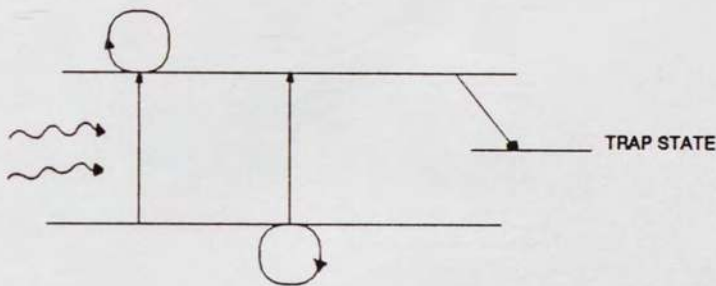
TWO STEP ABSORPTION

without relaxation at intermediate levels

(b)

with relaxation at intermediate levels

(c)

Figure 31. Possible mechanisms for darkening.

forward pump and probe, and backward pump and probe. The gratings were bleached out when a single beam was used to irradiate the sample. This was probably all the traps got filled destroying the spatial modulation.

The specific conclusions derived from our results can be summarized as following:

* At a given fluence and pulsewidth, darkening will always saturate to the same maximum level. The larger the fluence is, the greater this final maximum darkening level is.

* The dependence of darkening on repetition rate can be explained in terms of small recovery of darkening.

* The pulsewidth dependence suggests that the darkened glass is produced by a two step absorption process with a rapid (20-64 ps) decay for crossing between intermediate states. Two photon absorption and simple two step processes may be ruled out.

* The darkening cannot be healed with a high fluence He-Ne beam, nor can darkening be produced by intense near infrared (1.06 μm) pulses.

* Darkening is not bandgap resonant since several other glasses with different band gap darken by the same 532 nm beam.

4.2 Future Work

There is lot of scope for further experimentation. Darkening experiments could be carried out with a nanosecond laser. Spectrally resolved transmission change would be an interesting parameter to measure. This can be done by using a white light probe and examining its spectra. Darkening does not occur at near infrared (1.06 μm) wavelengths. It would be interesting to observe the threshold wavelengths at which darkening starts to appear.

LIST OF REFERENCES

[1] Neff, J.A. "Major initiatives for optical computing." Optical Engineering, 26, 7 (Jan 1987): 2.

[2] Huang, A. "Architechtural considerations ivolved in the design of an optical digital computer." Proceeding of IEEE, 72, 7 (July 1984): 780.

[3] Tanguay, A.R. "Materials requirements for optical processing and computing devices." Optical Engineering, 24, 1 (Jan/Feb 1985): 2.

[4] Smith, S.D., Janossy, I., MacKenzie, H.A., Reid, J.J.E., Taghizadeh, M.E., Tooley, F.A.P., Walker, A.C. "Nonlinear optical circuit elements as logical gates for optical computers: the first digital optical circuits." Optical Engineering, 24, 4 (July/Aug. 1985): 569.

[5] Smith, S.D., Walker, A.C., Wherrett, B.S., Tooley, F.A.P., Craft, N., Mathew, J.G.H., Taghizadeh, M.R., Redmond, I., Campbell, R.J. "Restoring optical logic: demonstration of extensible all-optical digital systems." Optical Eng., 26, (Jan 1987): 45.

[6] Goodman, J.W. Introduction to Fourier optics. New York: McGraw Hill, 1968.

[7] Gibbs, H.M., Jewell, J.L., Peyghambarian, N., Rushford, M.C., Tai, Tarang, S.S., Wiegmann, D.A. and Venkatesan, T.C. "Optical Bistability,Dynamical nonlinearity and Photonic Logic." Philos. Trans. R. Soc. London, A313, (March 1984): 245.

[8] Miller, D.A.B., Smith, S.D., and Johnson, A.M. "Optical bistability and signal amplification in a semiconductor crystal." Appl. Phy. Lett., 35, (1979): 658.

[9] Miller, A., Parry, G., and Daley, R. "Low power nonlinear Fabry-Perot Reflection in CdHgTe." IEEE J. Quantum Electron., QE-20, (1984): 7.

[10] Karpusho, F.V. and Sinitsyn,G.V. "Optical nonlinearity in ZnS." J. Appl. Spectros., 29 (1978).

[11] Taghizadeh, M.R., Janossy, I., and Smith, S.D. "Optical bistability in bulk ZnSe due to increasing absorption and self focussing." Appl. Phy. Lett., 46, 4 (1985): 331.

[12] Gibbs, H.M., McCall, S.L.,and Venkatesan, T.N.C. "Optical nonlinearity in Sodium." Phy. Rev. Lett., 36, (1976): 1135.

[13] Bischofberger, T., and Shen, Y.R. "Transient behaviour of anonlinear Fabry-Perot etalon." Appl. Phy. Lett., 32, (1978): 156.

[14] Jewell, J.L., Rushford, M.C., and Gibbs, H.M. "Use of a single nonlinear Fabry-Perot etalon as a logic gate." Appl. Phys. Lett., 43, 2 (1984): 175.

[15] Fisher, R.A. Optical phase conjugation. New York: Academic Press, 1983.

[16] Yariv, Amnon, and Yeh, P. Optical waves in crystal. New York: Wiley, 1984.

[17] Borelli, N.F., Hall, D.W., Holland H.J., and Smith, D.W. "Quantum confinement effects of semiconducting microcrystallites in glass." J. Appl. Phys., 61, 12 (June 1987): 5399.

[18] Potter, B.G., and Simmons, J.H. "Quantum size effects in optical properties of glass." Physical Review B, 37, 18 (June 1988): 10839.

[19] Jain, R.K.,and Lind, R.C. "Degenerate four-wave mixing in semiconductor-doped glasses." J. Opt. Soc. Am., 73, 5 (May 1983): 647.

[20] Rustagi, K.C., and Flytzanis, C. "Optical nonlinearities in semiconductor doped glasses." Optic Letters, 9, 8 (Aug 1984): 344.

[21] Roussignol, P., Ricard, D., Rustagi, K.C., and Flytzanis, C. "Optical phase cojugation in semiconductor-doped glasses." Optic communications, 55, 2 (Aug 1985): 143.

[22] Roussignol, P., Ricard, D., Lukasik, J., and Flytzanis, C. "New results on optical phase conjugation in semiconductor-doped glasses." J. Opt. Soc. Am. B, 4, 1 (Jan 1987): 5.

[23] Remillard, J.T., and Steel, D.G. "Narrow nonlinear-optical resonances in CdSSe-doped glass." Optic Letters, 13, 1 (Jan 1988): 30.

[24] Henesian, M.A., and Weber, M.J. "Nonlinear Absorption at 2ω (532 nm) and solarization in BK-7." private distribution.

[25] Mitsunga, M., Shinojima, H., and Kubodera, K. "Laser annealing effect on carrier recombination time in $CdS_x Se_{1-x}$ - doped glasses." J. Opt. Soc. Am. B, 5, 7 (July 1988): 1449.

[26] Hagen, W.F., and Snitzer, E. "Nonlinear solarization in Flint glasses by intense 0.53 μm light." International quantum electronics conference.

[27] Efros, Al.L., and Efros, A.L. Fiz. Tekh. Poluprovodn., 16, (1982): 1209. [Sov. Phys. - Semicond., 16, (1982): 772].

[28] Warnock, J., and Awschalom, D.D. "Electron confinement studies in colored glasses." Phys. Rev. B., 32, (1985): 5529.

[29] Chestnoy, N., Harris, T.D., Hull, R., and Brus, L.E. J. Phys. Chem., (to be published).

[30] Mansour, N., Canto, E., Soileau, M.J.,and Van Stryland, E.W. "Nonlinear Absorption initiated avalanche breakdown in dielectric ZrO_2." private distribution.

[31] Kwok, H.S., Zheng, J.P., Shi, L., Choa, F.S., Liu, P.L. "Intensity dependent photoluminiscent spectra of semiconductor doped glass." CLEO 88.

[32] Maxwell, J.C. Garnett Philos. Trans. R. Soc. London, 203, (1904): 385.

[33] Chemla, P.S., Miller, D.A.B., and Smith, P.W. Opt. Eng., 24, (1985): 556.